

Practical Homomorphic Aggregation for Byzantine ML

Antoine Choffrut
CEA LIST
Paris, France
antoine.choffrut@cea.fr

Rachid Guerraoui
Ecole Polytechnique Federale de
Lausanne (EPFL)
Lausanne, Switzerland
rachid.guerraoui@epfl.ch

Rafaël Pinot
Ecole Polytechnique Federale de
Lausanne (EPFL)
Lausanne, Switzerland
rafael.pinot@epfl.ch

Renaud Sirdey
CEA LIST
Paris, France
renaud.sirdey@cea.fr

John Stephan
Ecole Polytechnique Federale de
Lausanne (EPFL)
Lausanne, Switzerland
john.stephan@epfl.ch

Martin Zuber
CEA LIST
Paris, France
martin.zuber@cea.fr

ABSTRACT

Due to the large-scale availability of data, machine learning (ML) algorithms are being deployed in distributed topologies, where different nodes collaborate to train ML models over their individual data by exchanging model-related information (e.g., gradients) with a central server. However, distributed learning schemes are notably vulnerable to two threats. First, *Byzantine* nodes can single-handedly corrupt the learning by sending incorrect information to the server, e.g., erroneous gradients. The standard approach to mitigate such behavior is to use a non-linear robust aggregation method at the server. Second, the server can violate the privacy of the nodes. Recent attacks have shown that exchanging (unencrypted) gradients enables a *curious* server to recover the totality of the nodes' data. The use of homomorphic encryption (HE), a gold standard security primitive, has extensively been studied as a privacy-preserving solution to distributed learning in non-Byzantine scenarios. However, due to HE's large computational demand especially for high-dimensional ML models, there has not yet been any attempt to design purely homomorphic operators for non-linear robust aggregators. In this work, we present SABLE, the first completely homomorphic and Byzantine robust distributed learning algorithm. SABLE essentially relies on a novel plaintext encoding method that enables us to implement the robust aggregator over batching-friendly BGV. Moreover, this encoding scheme also accelerates state-of-the-art homomorphic sorting with larger security margins and smaller ciphertext size. We perform extensive experiments on image classification tasks and show that our algorithm achieves practical execution times while matching the ML performance of its non-private counterpart.

KEYWORDS

Homomorphic Encryption, Byzantine Machine Learning

1 Introduction

The quest for more accurate and versatile AI technologies has led machine learning (ML) researchers to considerably increase the complexity of the tasks they consider. As such, the size of learning models and datasets is increasing daily. To scale the computational resources and adapt to these new tasks, it is now common to rely on distributed methodologies in which the learning procedure is fragmented into several sub-tasks partitioned over different machines (a.k.a., *nodes*). The nodes execute their respective tasks in parallel and coordinate their actions, usually with the help of a central coordinator (a.k.a., *server*). Many distributed ML algorithms require the distribution of gradient computations across nodes, as in the renowned distributed stochastic gradient descent (DSGD) method [8]. In DSGD, the server maintains an estimate of the model which is updated iteratively by *averaging* the gradients computed by the nodes. However, as effective as it can be, distributed ML is also very vulnerable to *misbehaving* nodes. Indeed, a handful of nodes sending incorrect information (e.g., wrong gradients) can highly disrupt the learning procedure. Such a behavior can be caused by software and hardware bugs, poisoned data, or even by malicious players controlling part of the system. Following the terminology of distributed computing, these nodes are called *Byzantine* [42]. In the context of DSGD, Byzantine nodes may thus send erroneous gradients to the server, such as the negative of the true gradient. The presence of such nodes, which is arguably inevitable in real-world distributed settings, affects the trust in the efficacy of distributed ML solutions. Standard distributed learning algorithms, such as DSGD, completely fail to output accurate ML models in such an adversarial setting.

To mitigate the impact of Byzantine nodes in distributed learning, one can use a *robust* variant of DSGD, namely Robust-DSGD. The main modification to DSGD is to replace the averaging operation at the server by a *non-linear* robust aggregator. In fact, several such aggregation schemes have been proposed, such as coordinate-wise median (CWMED) [73], geometric median (GM) [16], coordinate-wise trimmed mean (CWTM) [73], Krum [9], among others. When choosing the robust aggregator in a suitable way, Robust-DSGD can be *proven* to be robust to Byzantine nodes, as described and analyzed in [4, 26, 38, 39]. Furthermore, this solution performs very well in practice against Byzantine attacks.

This work is licensed under the Creative Commons Attribution 4.0 International License. To view a copy of this license visit <https://creativecommons.org/licenses/by/4.0/> or send a letter to Creative Commons, PO Box 1866, Mountain View, CA 94042, USA.

Proceedings on Privacy Enhancing Technologies YYYY(X), 1–21

© YYYY Copyright held by the owner/author(s).

<https://doi.org/XXXXXXXX.XXXXXXX>



Yet, this scheme assumes that the central server is trusted. Third party servers are often operated by service providers, and one might reasonably assume that they seldom fail. However, the provider itself can be *curious*. One of the motivations of distributed learning is that nodes do not share their respective data, providing some level of sovereignty over their training datasets. However, exchanging gradients in the clear enables the server to infer sensitive information and sometimes even recover the totality of the nodes' data [27, 76, 79]. Therefore, it is of paramount importance to design solutions that, in addition to being robust to Byzantine nodes, also allow the honest nodes to protect their data against a *curious* server.

To overcome this problem, homomorphic encryption (HE) has been proposed as a privacy-preserving solution in distributed settings where clients attempt to offload part of their computations to a third party server. In particular, HE is receiving increasing attention from the ML research community [29, 37, 45, 48, 52, 61, 64]. In short, HE schemes allow certain mathematical operations (such as additions and multiplications) to be performed directly on encrypted data and without prior decryption. When decrypted, the output is the same as what would have been produced from the cleartext data. This property unlocks the use of HE schemes in distributed learning tasks for high-stake applications such as medicine and finance. Indeed, this enables several data providers to collaboratively train ML models with the help of a third party coordinator (a.k.a., server), without leaking any information to the server. For example, in DSGD, applying an *additive HE* scheme would allow an untrusted server to average encrypted gradients without compromising the privacy of the nodes. Previous works [65, 74] have demonstrated that homomorphic averaging could be performed on "large" models (500k parameters) with sub-1% computation overhead throughout the training. However, doing the same kind of efficient homomorphic adaptation to Robust-DSGD remains a very challenging task. The following question thus naturally arises.

Can we design an HE implementation of Robust-DSGD?

Answering this question boils down to overcoming the performance limitations of HE: while its costs are considered to be relatively low when implementing linear operations (such as averaging and summation), HE is notoriously much more computationally expensive when dealing with non-linear operations on high-dimensional data, which are at the core of Robust-DSGD. Indeed, HE schemes come with a limited set of (native) homomorphic operators, i.e., addition and multiplication, notably excluding comparison as well as division (even against cleartext values). Operations that one would consider elementary often offer a challenge in the encrypted domain to HE researchers. The crux is that HE schemes typically feature very few data structures and very limited flexibility to customize their size and shape to one's needs. In order to perform more elaborate operations beyond those native to the HE cryptosystem, one must design an algorithm implementing the desired operation together with an encoding of data into plaintexts that is amenable to this algorithm. Comparison operators, which are the essence of (non-linear) Byzantine resilient aggregators, constitute a perfect example of this challenge and have been the subject of a number of recent papers [15, 36, 66, 80].

Unfortunately, some of these solutions [36, 66] only allow a very limited set of homomorphic operations on ciphertexts *after the*

operation of comparison. These methods are therefore inadequate for the design of robust aggregators, which typically require much more complex operators such as *min/max* and *nearest neighbors* computations. Other works [15, 80] propose solutions that are only applicable to input vectors of small dimension and therefore are not suited in our case. This certainly makes their efficiency questionable when applied to modern-day and practically-relevant ML models where the number of parameters, i.e., the size of the gradients, can easily exceed the millions (or even billions). This inherent non-compliance of HE with non-linear operations in high dimensions introduces prohibitive computational costs when trying to homomorphically implement Byzantine robust aggregators.

In this work, we take a step into overcoming these challenges as we provide the first ever implementation of Robust-DSGD that is completely homomorphic. Furthermore, we perform extensive experiments on image classification tasks to test the efficacy and practical relevance of our algorithm. The next section describes our specific contributions in greater detail.

1.1 Our Contributions

We consider a distributed learning system comprised of n nodes and a server. We assume $f < n/2$ nodes are Byzantine (i.e., they may send any vector to the server), while the remaining nodes are honest (i.e., non-Byzantine). Furthermore, the server is considered to be *honest-but-curious*, i.e., the server correctly aggregates the nodes' vectors, but it would also use the received gradients to infer information about the nodes' data.

In this context, we propose a novel algorithm for Secure And Byzantine Robust LEarning, namely SABLE. To the best of our knowledge, this algorithm constitutes the first proposal of a homomorphic extension of DSGD that is robust to Byzantine nodes. SABLE incorporates the novel homomorphic robust aggregator HTS (Homomorphic Trimmed Sum), which we detail below, that simultaneously mitigates the impact of Byzantine nodes and provides strong cryptographic security ($\lambda \geq 128$).

Contrarily to previous approaches (see Section 2), SABLE does not leak any information on the nodes' data to the server, thereby preserving the privacy of the nodes. From a high level, in each iteration of SABLE, every node computes the gradient on a batch of its data, homomorphically encrypts the gradient, and then sends it to the server. The server then employs HTS to robustly aggregate the encrypted gradients, and sends the resulting ciphertext back to the nodes. Finally, the nodes decrypt the encrypted aggregate, and then locally update their estimate of the model parameters. Furthermore, to alleviate the in fine quadratic complexity of HTS, we feature in SABLE the option of *node subsampling*, whereby the server randomly selects a subset of the nodes and computes HTS only on their corresponding ciphertexts. This technique thus decreases the computational cost of the aggregation in the encrypted domain. We show in our work that node subsampling significantly improves the execution time of HTS (with no impact on the FHE security). Besides, by carefully tuning the number of nodes to be sampled, node subsampling yields similar empirical performances to SABLE in terms of ML accuracy and Byzantine resilience.

Technical challenges. First, we determine the most appropriate aggregator to implement homomorphically in terms of computational cost. We consider an exhaustive list of prominent robust aggregators from the literature, and qualitatively identify their major computational bottlenecks when implemented homomorphically. Our analysis promotes the coordinate-wise aggregators CWTM [73] and CWMED [73] for their inherent compatibility with batching-friendly FHE, a feature we argue is crucial for high-dimensional ML models. Indeed, batching allows many cleartext operations to be parallelized into single homomorphic computations, significantly amortizing their computational cost. Finally, we choose CWTM (coordinate-wise trimmed mean) as the main robust aggregator to be used in SABLE due to its theoretical and empirical superiority in ML performance [4, 26]. Note that due to space limitations, we defer the full analysis to Appendix B.

Second, we introduce HTS (Homomorphic Trimmed Sum), which is the first attempt at computing CWTM homomorphically. The design of HTS poses a number of challenges. While batching can help to implement CWTM homomorphically, it is not sufficient on its own as CWTM requires a sorting operation which is notoriously costly to perform in the encrypted domain. Indeed, some batching-friendly homomorphic sorting operators have been proposed in the literature [36, 51, 66], however they cannot be directly used for CWTM which calls for the addition of a selection of elements *after* they have been sorted. In fact, the encoding of integer values into plaintexts in these solutions is ill-adapted to our problem. To circumvent this limitation, we devise a novel plaintext encoding method that exploits an extra degree of freedom in HE schemes (specifically, we decouple the base in the integer decomposition from the plaintext modulus). This serves multiple purposes simultaneously: (1) it allows to customize data structures that are better adapted to the dimension of vectors and the range of their values; (2) it reduces the multiplicative depth of the homomorphic circuits and the computational time of their execution; and (3) it offers better security margins. The upshot is that with this extra degree of freedom, we are able to implement CWTM homomorphically, while it was either impractical [15, 80] or out of reach [36, 66] with existing solutions, and with better performance and security than one could have hoped for. As an interesting special case of HTS, we also obtain a homomorphic implementation of CWMED which we call HMED, without incurring additional computational costs.

Empirical evaluation. We thoroughly test the performance of our algorithm both in terms of computational cost and learning accuracy. Indeed, we implement SABLE on benchmark image classifications tasks with large models, and provide unit execution times of our implementation. Our results show that HTS has practical execution times, especially when distributing the computations at the server across several cores. Furthermore, node subsampling significantly accelerates the computations, with a speedup of up to 9× in certain settings. Moreover, we test SABLE, purely in terms of ML performance, in two distributed systems and under different Byzantine regimes. Our experiments show that SABLE is consistently robust to Byzantine attacks and matches the performance of its non-private counterpart Robust-DSGD on MNIST [22] and CIFAR-10 [41], even when using small bit precisions (see Section 6). This demonstrates the practical relevance of our algorithm.

1.2 Paper Outline

The remainder of this paper is organized as follows. Section 2 discusses the different frameworks that we believe to be related to our work. Section 3 contains background information on Byzantine ML and HE needed to understand the paper, and presents the CWMED and CWTM aggregators. Section 4 introduces our novel operator HTS and shows its improvements over the state-of-the-art. Section 5 presents SABLE, while Section 6 evaluates its performance on benchmark ML tasks. Finally, Section 7 presents concluding remarks. For ease of reading, we also include a list of notations in Appendix A.

2 Related Work

In the past, significant progress has been made in addressing the concerns of data privacy and Byzantine robustness separately in distributed learning. Indeed, several works [46, 52, 55, 67, 74] study the use of HE to enhance the privacy of distributed learning when all nodes are honest (e.g., DSGD, federated learning). Similarly, [10] have used secure multi-party computation (MPC) to make federated averaging privacy-preserving *in the absence of Byzantine nodes*. However, this Byzantine-free scenario is over-idealistic as it does not take into account node faults that occur often in practical systems. On the other hand, [4, 26, 39] among others have developed Byzantine resilient algorithms for distributed learning with meaningful convergence guarantees. Yet, these works do not consider the major privacy risk that ensues from sending the gradients in the clear to the server [27, 76, 79].

Recently, there have been several attempts to simultaneously tackle the notions of privacy and Byzantine robustness in distributed learning. For example, [5, 30, 78] investigate the use of differential privacy in Byzantine resilient learning algorithms to protect the privacy of the nodes against the server. These techniques usually rely on injecting noise into the gradients of the nodes. While these schemes provide strong privacy guarantees, it is usually at the expense of accuracy as noise injection introduces a significant trade-off between utility and privacy [28]. Furthermore, standard techniques for differential privacy seem to conflict with the theoretical guarantees of Byzantine robustness, considerably reducing the practical relevance of the scheme [5, 30].

Some works [50, 77] suggest using hardware-based solutions such as trusted execution environments (e.g., Intel SGX) to prevent the server from seeing the data. However, these solutions rely on trusted dedicated hardware.

Other works [21, 33, 34, 40, 53, 63, 68, 75] make use of secure MPC to protect the privacy of the nodes. However, [21, 33, 34, 40, 53, 75] assume the presence of two non-colluding honest-but-curious servers in the system, which is notoriously known for being a much stronger assumption than the single server setting that we consider. Furthermore, the solutions of [34, 63] do not protect the pairwise distances between model updates of honest nodes, that are leaked to the servers, hence constituting a significant privacy breach. Additionally, [33] uses a Byzantine robustness model based on FLTrust [13], which requires the server to possess a clean trusted dataset. This relies on the strong assumption that the server has access to additional knowledge to filter out Byzantine nodes, rather than only using the nodes' gradients as done in our work. Moreover,

the Byzantine resilient approach proposed in [68] tolerates a smaller number of Byzantine nodes in the system and makes non-standard ML assumptions (e.g., bounded node updates).

Finally, a handful of prior works [47, 49, 59, 69] actually investigate the use of HE to grant privacy to Byzantine robust ML algorithms. The previous work closest to ours [69] attempts to implement the Multi-Krum [9] aggregator using the additively homomorphic Paillier cryptosystem in a blockchain-based infrastructure. However, their approach does not fully implement Multi-Krum in the encrypted domain in order to fit the constraint of that cryptosystem. In turn, this solution induces significant leakage towards the aggregation nodes (equivalent to the server in our setting), hence significantly diminishing the privacy of the solution. Additionally, in the solution proposed in [59], the server has access to the resulting model at every step of the algorithm, also endangering the privacy of the nodes. On the other hand, [47, 49] combine HE with weaker notions of Byzantine robustness. Indeed, [49] uses the FLTrust robustness model (mentioned above), while [47] homomorphically implements Robust Stochastic Aggregation (RSA) [43], a robust variant of SGD. However, RSA has weak theoretical guarantees: it is only proven for strongly convex functions (which is seldom true for modern neural networks), and it provides sub-optimal guarantees as it does not employ noise reduction techniques (Theorem 2 in [38]).

In contrast, our work uses a state-of-the-art Byzantine robustness model, uses only HE as a security primitive, and does not leak any private information to the curious server.

3 Model Setting and Preliminaries

In this section, we present background information needed to understand the paper. Specifically, we start by presenting the standard Robust-DSGD protocol (Algorithm 1) in Section 3.1, and discuss its robustness guarantees against Byzantine nodes. Then, we introduce the concept of HE in Section 3.2, and the BGV cryptosystem we use to design HTS in Section 3.3. Finally, in Section 3.4, we present the coordinate-wise aggregators CWMED and CWTM.

3.1 Distributed Byzantine Learning

We consider a distributed architecture composed of n nodes and an honest-but-curious server. Every node i has a local dataset D_i . Furthermore, we assume the presence of $f < n/2$ Byzantine nodes in the system.¹ Following the terminology of Byzantine ML [4, 26, 38], Byzantine nodes *only* aim to disrupt the algorithm in terms of ML performance by sending erroneous vectors to the server, i.e., they do not deviate from the rest of the protocol. The remaining $n - f$ nodes are considered to be correct (a.k.a., honest), and follow the prescribed protocol exactly. The objective of the honest nodes is to train a joint ML model over the collection of their individual datasets with the help of the server, despite the presence of Byzantine nodes.

As shown in [9], the averaging operation at the server in DSGD is arbitrarily manipulable by a single Byzantine gradient. This renders the underlying algorithm vulnerable to Byzantine nodes, making it impossible for honest nodes to build an accurate ML model. Consequently, recent works proposed a robust variant of DSGD, that we call Robust-DSGD [4, 26, 38, 39], described in Algorithm 1. In

summary, Robust-DSGD enhances the robustness of DSGD by incorporating two additional features. First, instead of sending the gradients directly to the server, the honest nodes first compute the Polyak’s momentum [58] on their gradients. Second, the averaging operation at the server is replaced by a more complex Byzantine resilient aggregator F . F is designed to aggregate the nodes’ momentums in a way that would mitigate the attacks launched by Byzantine nodes (in the form of incorrect gradients).

Algorithm 1 Robust-DSGD

► Initial model θ_0 , learning rate γ , initial momentum $m_0^{(i)} = 0$ for each honest node i , momentum coefficient $\beta \in (0, 1)$, robust aggregation F , and number of steps T .

- 1: **Server** sends θ_0 to all nodes
- 2: **for** $t = 1, \dots, T$ **do**
- 3: **Every honest node** i **does in parallel**
- 4: Compute gradient $g_t^{(i)}$ on θ_{t-1}
- 5: Compute momentum $m_t^{(i)} = \beta m_{t-1}^{(i)} + (1 - \beta)g_t^{(i)}$
- 6: Send $m_t^{(i)}$ to **Server**
- 7: **end block**
- 8: **Server** aggregates $M_t = F(m_t^{(1)}, \dots, m_t^{(n)})$
- 9: **Server** updates the model locally $\theta_t = \theta_{t-1} - \gamma M_t$
- 10: **Server** sends new model θ_t to all nodes
- 11: **end for**
- 12: **Every honest node** i returns θ_T

However, the aggregation method F must be chosen carefully. Indeed, only a specific subset of methods has been proven to confer theoretical robustness guarantees to Algorithm 1 [4, 26]. This subset comprises the following aggregations: *Krum* (and *Multi-Krum*) [9], *geometric median* (GM) [17], *minimum diameter averaging* (MDA) [23], *coordinate-wise trimmed mean* (CWTM) [73], *coordinate-wise median* (CWMED) [73], and *mean-around-median* (MeaMed) [71]. For example, when setting $F = \text{CWTM}$ in Robust-DSGD, the model converges at the rate $O\left(\frac{f}{nG^2} + \sqrt{\sigma^2(f+1)/Tn}\right)$, where σ^2 is the stochastic variance when sampling gradients, G^2 measures the inherent heterogeneity in the datasets of honest nodes, and T is the number of steps.² Besides offering theoretical guarantees, these robust methods are shown to empirically mitigate state-of-the-art Byzantine attacks, when combined with momentum [4, 24, 26].

Therefore, our objective in this work is to design an HE-based version of Robust-DSGD, where the aggregator F is implemented completely in the homomorphic domain. Despite the existence of other robust methods in the literature (e.g., CGE [31] and CC [38]), we only consider resilient aggregators that possess theoretical guarantees ensuring the convergence of Algorithm 1 in the presence of $f < n/2$ Byzantine nodes.

3.2 Homomorphic Encryption for ML

Just like any other cryptosystem, a *Homomorphic Encryption* (HE) scheme comes with an *encryption* operator which transforms a

¹Otherwise, no meaningful learning guarantees can be obtained [44].

²This rate is optimal in terms of asymptotic error [4, 39].

plaintext pt into a ciphertext ct with the help of a public encryption key pk . *Decryption* is the process of recovering the plaintext from the ciphertext ct using the secret key sk associated to pk .

The specificity of HE systems is that they offer the option of performing certain operations on ciphertexts, without access to the decryption key. Essentially, after performing the operation on the encrypted data, decryption returns the same value as if the original plaintext had been processed directly. Such an operation on plaintexts and its counterpart on ciphertexts are said to be *homomorphic*. More formally,

$$\text{Decr}_{sk}(h(ct_1, \dots)) = h(\text{Decr}_{sk}(ct_1), \dots) \quad (1)$$

where ct_1, \dots are ciphertexts, and h is overloaded to denote both the operation on plaintexts and ciphertexts.

An HE scheme comes with a fixed, hence fairly rigid structure for plaintexts and a limited toolbox of core homomorphic operations. Accordingly, native homomorphic operations generally do not go much beyond addition and multiplication³. Although Turing-complete, a direct use of this bare-bones formalism generally leads to prohibitive performances for most practical applications. Part of the work of the HE community goes into designing efficient algorithms and tailoring a suitable encoding of data into plaintexts to extend the native toolbox.

In current ML tasks, models are increasing in complexity by the day, i.e., the number of model parameters grows due to the large-scale availability of data. This implies that nodes in distributed learning systems would compute (and exchange) gradients of significant size. Given that HE is quite expensive when performing non-linear operations (a crucial pillar of Byzantine robustness) in high dimensions, we would like to use an FHE cryptosystem that possesses batching capabilities in order to benefit from this parallelization of computations when encrypting gradients. This would significantly amortize the execution times of homomorphic operators. Furthermore, since FHE operators generally induce large computational and communication costs, we consider a cross-silo architecture with a relatively small number of nodes (not exceeding 15) while tolerating large ML models.

FHE generally refers to several cryptosystem families. The first family is that of "practically true" FHE cryptosystems, meaning schemes with a practical bootstrapping procedure. So far, TFHE [19] is the only member of that family. While able to efficiently compute distances on small sets of low-dimensional vectors and having a programmable bootstrapping well suited for non-linear operations, TFHE does not offer large plaintext domains (e.g., it is typically limited to \mathbb{Z}_{16}) and does not support batching. The absence of these two critical properties, given the large number of dimensions of current ML models, makes TFHE a priori less suitable for this work.

The other family of FHE cryptosystems is the class of *somewhat homomorphic encryption* (or SHE), including BGV [12], BFV [11, 25], and CKKS [18]. These cryptosystems have a larger plaintext domain (see Section 3.3 for details), meaning that they can pack a number of integers⁴ into a single ciphertext. As a result, the homomorphic operators apply independently on all these integers in a SIMD (Single Instruction Multiple Data) parallel fashion. This means that

cryptosystems in this family generally lead to acceptable *amortized* costs for applications that need to apply a given algorithm to many inputs in parallel. The parallelization and batch-friendliness properties of SHE schemes makes BGV, BFV, and CKKS desirable candidates for the cryptosystem to be used. In this work, we use the **BGV** cryptosystem and present it in Section 3.3. More details on our choice of cryptosystem can be found in Appendix B.

3.3 The BGV Cryptosystem

We refer the reader to [12] for notation and a more thorough description of the algebraic structures involved in BGV.

The plaintext space. The plaintext space in BGV is the modular polynomial ring $\mathbb{Z}_p[X]/\langle\Phi_m(X)\rangle$, where p is the *plaintext modulus* and $\Phi_m(X)$ is the *cyclotomic polynomial* of index m . The degree of this polynomial is given by Euler's totient function $\varphi(m)$, returning the number of integers up to m that are relatively prime to it. Note that $\varphi(m)$ can be fiddly to work with analytically and for simplicity, we will choose a prime m where $\varphi(m) = m - 1$ in the sequel. In essence, a plaintext is a (typically very long) polynomial with $\varphi(m)$ coefficients taken in the interval $\{0, \dots, p - 1\}$. Arithmetic operations on polynomials are performed modulo $\Phi_m(X)$, and arithmetic operations on their coefficients are performed modulo p .

The ciphertext space. The ciphertext space is of the form $\mathbb{Z}_q[X]/\langle\Phi_m(X)\rangle$, where $\Phi_m(X)$ is the same as in the plaintext space, but the *ciphertext modulus* q is chosen much larger than p to ensure correctness. Actually, a BGV instance comes with a *family* of ciphertext spaces, but for the purposes of our discussion, there is no harm in assuming that there is only one. The interested reader can inquire about the ciphertext modulus chain in [12].

Batching. BGV comes with a natural plaintext encoding scheme, performed via the *Number Theoretic Transform* (NTT) [57] and referred to as *batching*. Batching takes place prior to encryption and encodes a vector v of d polynomials $s^{(i)}$ of equal length N , called *slots*, into a plaintext polynomial pt :

$$v = (s^{(0)}, \dots, s^{(d-1)}) \rightarrow \boxed{\text{Batch}} \rightarrow pt \quad (2)$$

where N is the multiplicative order of p modulo m and satisfies $\varphi(m) = dN$. The upshot is that addition and multiplication of vectors are performed slot-wise via suitable operations on the associated plaintexts thanks to the Chinese Remainder Theorem. Polynomial operations are thus parallelizable in a SIMD fashion.

HE on vectors of slots. To the extent that the basic objects are now vectors of slots, and not plaintexts themselves, we need to revisit the notion of homomorphic operators. This notion now relates to operators on vectors of slots and on ciphertexts, via the composite transformation of batching and encryption:

$$v \rightarrow \boxed{\text{Batch}} \rightarrow pt \rightarrow \boxed{\text{Encr}_{pk}} \rightarrow ct \quad (3)$$

An operator on vectors of slots is said to be *homomorphic* if there exists an operator on the associated ciphertexts which results in the same value upon decryption. In other words,

$$\begin{aligned} & \text{Batch}^{-1} \circ \text{Decr}_{sk}(h(ct_1, \dots)) \\ &= h(\text{Batch}^{-1} \circ \text{Decr}_{sk}(ct_1), \dots) \end{aligned} \quad (4)$$

³TFHE's functional bootstrapping operation stands apart in this respect.

⁴Real-valued gradient coefficients can thus be adequately represented by rescaling.

where h now denotes both the operator on vectors of slots and on the corresponding ciphertexts.

Slot-wise homomorphic operators. Certain homomorphic operators in BGV work slot-wise in their inputs. All homomorphic operators introduced in this paper are a composition of three such operators: addition, multiplication, and the coefficient extraction operator defined by

$$\text{Ext}_i(v) := \left(\text{Ext}_i(s^{(0)}), \dots, \text{Ext}_i(s^{(d-1)}) \right) \quad (5)$$

where for $i \in \{0, \dots, n-1\}$ and $j \in \{0, \dots, d-1\}$, $\text{Ext}_i(s^{(j)})$ is a constant-coefficient slot containing the i -th coefficient of slot $s^{(j)}$.

Noise. BGV is part of a family of schemes whose security is based on the hardness of the so-called RLWE problem. Such schemes require the addition of noise at encryption time, this noise amplifies during homomorphic operations especially multiplications. Decryption may then fail to remove the noise when it is too large, resulting in erroneous cleartexts. In practice, a useful metric for the total noise growth occurring in a circuit is its *multiplicative depth*, which denotes the maximum number of *successive* multiplications performed on any ciphertexts in the circuit.

Parameter selection in BGV. The choice of m , plaintext modulus p , and ciphertext modulus q is far from trivial as they have complex and conflicting effects on *security*, *correctness*, *time performance*, and *data encoding*. Parameterizing BGV to simultaneously achieve these objectives is thus not completely straightforward.

- *Security.* The security level λ is chosen above 128 bits as is standard practice in the field [1]. In practice, λ increases as $\varphi(m)$ increases, decreases as q increases and increases with the variance of the noise [2]. Although $\varphi(m)$ and q change throughout our experiments, the variance of the noise is set to a standard value of 3.2 [1] and is never changed as is common practice.
- *Correctness.* The ratio q/p controls how far plaintexts are spread apart in the ciphertext space during encryption, and thus the security level of the instance. It also fixes a bound on the multiplicative depth of the circuit that the BGV instance will be able to correctly decrypt. While p mainly plays a role in the encoding of data into plaintexts and the algorithm's complexity, increasing q aims precisely to accommodate for the total noise growth that will result from the operations.
- *Time performance* increases with the degree $\varphi(m)$ of ciphertext polynomials and the size of their coefficients taken in the range $\{0, \dots, q-1\}$. The complexity of parametrization is compounded by the fiddly dependency of $\varphi(m)$ on m .
- *Encoding.* The degree N of each slot is given by the multiplicative order of p modulo m and the number of slots is then $d = \varphi(m)/N$. In principle, each slot has the maximum capacity to encode values in the range $\{0, \dots, p^N - 1\}$. However, the choice of the precise encoding has far reaching consequences on the complexity and multiplicative depth of the circuit. This is precisely one of the main contributions of this paper, as we explain in Section 4.1.

REMARK 1. *Batching in BGV only requires that p be prime and not divide m . In several current implementations of BGV [6, 60], the choice of m as a power of 2 is either imposed or the default, and when batching is used, p is taken such that $N = 1$, thus imposing slots of size 1. In contrast, the HELib [32] library does not impose such*

restrictions and leaves freedom to search for the values of m and p yielding optimal values for N and d . Because we need this flexibility in our algorithm, we use HELib (version 2.2.0) in our work to implement our homomorphic operators. Although our work could be implemented in theory using BFV, we have limited our experimentation to BGV as HELib only implements BGV and CKKS.

3.4 FHE-compliance of Byzantine Aggregators

We qualitatively review six prominent Byzantine aggregators with respect to their compliance with the mainstream FHE cryptosystems in terms of evaluation cost. We classify these operators into two categories. First, we have geometric approaches which select one or more vectors based on a global criterion, but which are subject to a selection bottleneck in high dimensions. This makes these approaches difficult to implement efficiently in the homomorphic domain when dealing with high-dimensional ML models. Second, coordinate-wise approaches, which manipulate each coordinate independently, appear to be the most promising due to their inherent compliance with batching-friendly FHE cryptosystems, in particular those with a static selection criterion. Our analysis promotes the use of the coordinate-wise aggregators CWMED and CWTM, which we present here. Due to space limitations, we defer the complete analysis of the FHE-compliance of the six prominent Byzantine aggregators to Appendix B.

Coordinate-wise aggregators. These methods are intrinsically batching-friendly since all vector coordinates can be processed independently. These approaches are therefore a priori promising candidates to be implemented over BGV or any other batching-able FHE scheme. In fact, their homomorphic evaluation would scale well to large models, thanks to both the SIMD parallelism available in each ciphertext and the fact that many such ciphertexts can be straightforwardly processed in parallel.

- *Coordinate-Wise Median (CW MED)* [73]. Median calculations have recently been studied over batching-friendly cryptosystems [36]. However, computing a median even over a small number of values requires large computational times. For example, [36] reports that a median over 16 8-bit vectors of size 9352 takes around 1 hour. The *amortized* time per component appears more reasonable (≈ 0.38 s). These results are promising (by FHE standards) and hint that more practical computational times may be obtained using further optimizations or by decreasing the precision of the vectors and/or the number of inputs.
- *Coordinate-Wise Trimmed Mean (CWTM)* [73]. This method performs a coordinate-wise sorting and then averages the $(n-2f)$ coordinates between positions f and $n-f-1$.⁵ Specifically, given n vectors x_0, \dots, x_{n-1} of dimension d , CWTM sorts the n vectors per coordinate to obtain $\bar{x}_0, \dots, \bar{x}_{n-1}$ satisfying

$$\bar{x}_0^{(j)} \leq \dots \leq \bar{x}_{n-1}^{(j)} \quad 0 \leq j \leq d-1, \quad (6)$$

and returns the vector y such that

$$y = \frac{1}{n-2f} \sum_{i=f}^{n-f-1} \bar{x}_i \quad (7)$$

⁵Recall that n is the total number of nodes, and f is the number of Byzantine nodes.

This operator should have similar cost to CWMED, since the selection is replaced by an averaging over statically selected coordinates and summation is generally a low-cost homomorphic operation. Note that since divisions are quite impractical in the homomorphic domain, the averaging operation in CWTM can be replaced by a homomorphic summation followed by a post-decryption division on the nodes' side. There is no added value in terms of security to perform the division prior to the decryption as the number of nodes is a public information.

Be it for the trimmed mean or the median, the algorithm in the encrypted domain requires to sort the values and compute their ranks. Since data-dependent branching is not possible in a homomorphic setting, all pairs of values must be compared, thus yielding quadratic complexity. Also, in both algorithms, the rank of all elements must be homomorphically determined in order to decide which ones enter the final computation. In other words, both algorithms exhibit the same computational complexity and multiplicative depth.

From an ML viewpoint, these two popular methods have been shown to provide state-of-the-art Byzantine robustness [26, 38, 39]. Furthermore, CWTM has been shown to be empirically and theoretically superior to CWMED in [4]. As such, we choose in this work to achieve Byzantine resilience via a homomorphic implementation of CWTM over the BGV cryptosystem.

4 HTS: Homomorphic Trimmed Sum

In this section, we introduce HTS, a homomorphic implementation of CWTM (up to a publicly known scaling factor) over BGV given in (6) and (7). As previously mentioned, for efficiency purposes, we offload the division by $(n - 2f)$ at the end of CWTM (see (7)) to the nodes' side and thus implement a slightly modified version of CWTM. We also obtain the median operator as a special case in (15). In our algorithm design, we exploit an extra degree of freedom in the parameters, which enables us to (i) fully optimize the batching capabilities of the BGV scheme; (ii) reduce the multiplicative depth of our circuit; and (iii) handle additional operations, beyond comparisons, such as the sum around the median in CWTM. To the best of our knowledge, none of the existing implementations achieves these three objectives simultaneously.

REMARK 2. *The BGV scheme naturally manipulates integer values but can also handle fixed-precision values by scaling them and encoding them as integers, as long as the algorithm tolerates these precision errors (an issue which is more often than not overlooked by the FHE community). This is the case for CWTM and CWMED, as they only select input values (with an additional summation for CWTM).*

4.1 Plaintext Encoding Method

Since slots, which are the elementary objects in the BGV scheme with batching, are polynomials, a reasonable choice for the encoding of an integer a is to write it in the form

$$a = \sum_{i=0}^{N-1} c_i B^i \quad (8)$$

where B is the base, N is the length of the digit decomposition, and the digits c_i must satisfy $0 \leq c_i < B$. The integer a can be mapped

to the slot $s = \sum_{i=0}^{N-1} c_i X^i$ provided $B \leq p$ and N coincides with the number of coefficients in each slot (see the discussion around (2) for notation). Since a slot's coefficients are taken modulo p , a common inclination is to take $B = p$, in which case each coefficient has the capacity to encode the set $\{0, \dots, p-1\}$ and thus a slot has the capacity to encode the set $\{0, \dots, p^N-1\}$. This is adequate in certain applications, for example a single comparison in the bivariate approach [36, 66]. Unfortunately, this precludes even a single addition of ciphertexts as the resulting coefficients in a slot will typically overflow the range $\{0, \dots, p-1\}$. This problem arises precisely in the univariate approach of the comparison operators, where the *difference* on the digits of the slots is tested for negativity. To remedy this, [36, 51, 62] take $B = (p-1)/2$. These implementations are only adequate for simple comparisons, min/max, sorting, as well as one addition of two ciphertexts. However, they cannot handle CWTM as it generally involves at least two additions.

Decoupling B from p . These observations have led us to reconsider the role of the plaintext modulus p in the design of encoding schemes. Our main insight is that p does not have an intrinsic interpretation as the base B , but merely imposes the restriction that $B \leq p$. Attention should be focused on exploiting the batching capabilities of the BGV scheme and on reducing the multiplicative depth and complexity of the homomorphic operators, rather than on making the best of a slot's storage capacity. As explained in Section 3.3, the ciphertext modulus q , not the plaintext modulus p , directly impacts performance. Certainly, a larger p increases the noise added by each operation, but the tradeoff is not in favor of minimizing p as is illustrated by our experiments in Table 1.

In conclusion, our approach is to decouple the base B from the plaintext modulus p . This is an extra degree of freedom that we have not seen exploited in the literature so far. In order to represent the range $\{0, \dots, M-1\}$ for some integer M , our method chooses a base B and length N so that B^N is as close to M as possible. Note that the complexity and multiplicative depth of homomorphic functions operating on the slots' coefficients can be reduced with a smaller B . On the other hand, with a larger N , more work is required to reassemble the coefficient-wise results to obtain the final slot-wise results. But since $N \approx \log M / \log B$, B can be quite significantly reduced without increasing N too much. Once B and N have been optimized, our method searches values for m , p , and q achieving N while satisfying a minimum security level of 128 bits (recall discussions around (2) and (8) for notations). Since B is now decoupled from p , we have a lot more freedom to perform the two optimizations one after the other.

4.2 Homomorphic Comparison Operators

Integers $a = \sum_{i=0}^{N-1} c_i B^i$ and $a' = \sum_{i=0}^{N-1} c'_i B^i$ decomposed according to (8) can be ordered via the lexicographic ordering on their digits with the formula

$$\mathbf{1}(a < a') = \sum_{i=0}^{N-1} \left(\mathbf{1}(c_i < c'_i) \times \prod_{j=i+1}^{N-1} \mathbf{1}(c_j == c'_j) \right), \quad (9)$$

where $\mathbf{1}(\text{true}) = 1$ and $\mathbf{1}(\text{false}) = 0$. We then define the slot-wise *less-than operator* LT, satisfying $\text{LT}(v, v') = \mathbf{1}(v < v')$ where

v and v' are vectors of slots, with

$$\text{LT}(v, v') := \sum_{i=0}^{N-1} \left(\text{Neg}(\text{Ext}_i(v) - \text{Ext}_i(v')) \right) \quad (10)$$

$$\times \prod_{j=i+1}^{N-1} \text{Zero}(\text{Ext}_j(v) - \text{Ext}_j(v'))$$

where Ext_i are the coefficient extraction operators introduced in (5), Zero is the (slot-wise extension of the) Lagrange polynomial operator satisfying $\text{Zero}(c) = \mathbf{1}(c == 0)$ for $-B+1 \leq c \leq B-1$, and Neg is the (slot-wise extension of the) Lagrange polynomial operator satisfying $\text{Neg}(c) = \mathbf{1}(c < 0)$ for $-B+1 \leq c \leq B-1$.

REMARK 3. *The impact of decoupling B from p becomes clearer from the structure of our operators Zero and Neg . While previous work (e.g., [36, 66]) uses polynomials of degree $p-1$, here Zero and Neg are implemented as polynomials of degree $2B-1$. The complexity and multiplicative depth of these operators alone can be significantly reduced by lowering B .*

The comparison operator Comp . Instead of testing for $\mathbf{1}(v < v')$ for all pairs of vectors v and v' , following a device from [14], we introduce⁶ the (homomorphic) operator

$$\text{Comp}(v, v'; i, j) = \begin{cases} \text{LT}(v, v') & \text{if } i \geq j \\ 1 - \text{LT}(v', v) & \text{if } i < j \end{cases} \quad (11)$$

It handles elegantly the likely situation where values are repeated by flagging them when they appear later in the list.

The rank operator rk . Given a list of vectors v_0, \dots, v_{n-1} , we compute their respective ranks $\text{rk}_0, \dots, \text{rk}_{n-1}$, producing a reordering of the range $\{0, \dots, n-1\}$ satisfying

$$\begin{cases} \text{rk}_i < \text{rk}_j & \text{if } v_i < v_j, \\ \text{rk}_i \neq \text{rk}_j & \text{if } v_i == v_j \text{ and } i \neq j. \end{cases} \quad (12)$$

This echoes (6). Such an operator rk is given by

$$\text{rk}_i := \sum_{j=0}^{n-1} \text{Comp}(v_i, v_j; i, j) \quad (13)$$

In the next section, we introduce HTS, our implementation of the coordinate-wise trimmed sum operation.

4.3 The HTS Operator

We note that existing solutions from the literature could have alternatively been used to build homomorphic implementations of the less-than, comp, and rank operations. Yet, we have argued that our method offers improved performance and this is amply illustrated and discussed in Section 4.4. In contrast, the coordinate-wise trimmed sum operation, namely the sum in the right-hand side of (7), is out of reach for existing solutions prior to our work as already argued in Section 4.1.

Echoing (7), our homomorphic trimmed sum operator is:

$$\text{HTS}(v_0, \dots, v_{n-1}; f) := \sum_{i=0}^{n-1} \text{Btw}(\text{rk}_i; f, n-f-1)v_i \quad (14)$$

⁶Note that this operator Comp is not the same as that from [14] or that used in [36] since they encapsulate different operators for the less-than operation (LT).

where, suppressing a dependency on n , $\text{Btw}(\cdot; f, n-f-1)$ is the Lagrange polynomial satisfying

$$\text{Btw}(\text{rk}; f, n-f-1) = \mathbf{1}(\text{rk} \in \{f, \dots, n-f-1\}), \quad \text{rk} \in \{0, \dots, n-1\}$$

and is hence of degree n . Looking at (13)–(14), this algorithm is quadratic in complexity in the number of inputs n . The homomorphic median operator is a special case of HTS where only the value with rank $\lfloor n/2 \rfloor$ is selected:

$$\text{HMED}(v_0, \dots, v_{n-1}) = \text{HTS}(v_0, \dots, v_{n-1}; \lfloor n/2 \rfloor) \quad (15)$$

Since the complexity and multiplicative depth of $\text{Btw}(\cdot; f, n-f-1)$ are independent of f , HTS and HMED have equal complexities and multiplicative depths.

4.4 Performance of HTS

This section illustrates the gain in performance when using our method for the task of homomorphic sorting compared to the current state-of-the-art algorithm [36], see Table 1. Experiments are run on the same machine.⁷ For the purpose of illustration, we have chosen to present evaluations of coordinate-wise sorting over $n = 4$ vectors with 8-bit coordinates and dimension $d = 9352$ and 5764. This choice of values is justified below. In every setting, q is optimized to be as small as possible while still ensuring correctness. The security level is evaluated in bits and obtained using the latest commit of the lattice estimator⁸ [2].

Algo	m	p	q (bits)	λ (bits)	Am. Time (ms)	Am. Size (Bytes)
[36]	28057	167	410	166	5.6	308
Ours	28057	167	300	238	4.8 (1.2×)	225 (1.4×)
[36]	17293	131	360	106	4.6 (1.2×)	270 (1.1×)
Ours	17293	131	280	152	3.8 (1.5×)	210 (1.5×)

Table 1: Speed-up of our method compared to [36] when evaluating a coordinate-wise sorting over 4 vectors of 8-bit coordinates. For each method, the optimum q is reported. The amortized (Am.) time and size per coordinate are also shown. We display the amortized time as it allows an absolute comparison, regardless of the dimension of the vectors. The improvement (×) in time and size with respect to the first row is also reported in the respective columns. The red value 106 highlights a weak bit security ($\lambda < 128$).

The first line of the table shows the results of our implementation of [36]’s sorting algorithm using the parameters given in their paper ($m = 28057$ and $p = 167$, for which $d = 9352$ and $N = 3$, see Table 3 [36]). Using the same parameters m and p (and thus the same d and N) but a significantly smaller $B = 7$, the second line shows how our method significantly decreases q thanks to the reduced multiplicative depth of our algorithm. This results in a higher security level λ for our solution (236 bits) and a 1.2× gain in computational performance over the other method. Since our method provides a substantial increase in the security level, in the fourth line we use a lower value for m in order to push the security

⁷Machine with a 12th Gen Intel® Core™ i7-12700H processor with 62.5GiB memory using a single core.

⁸https://lattice-estimator.readthedocs.io/en/latest/readme_link.html

level down closer to the standard 128 bits. We take $m = 17293$ and $p = 131$, for which $d = 5764$ and $N = 3$ (recall (2)), thus achieving a security level similar to the one in the first line, and with $B = 7$ we gain a $1.5\times$ speed-up. As an added bonus, the smaller value for q that the flexibility of our method incurs also leads to smaller ciphertexts. Indeed, we show in Table 1 that our ciphertexts are $1.5\times$ smaller in size than the ciphertexts in previous works.

The third line shows the results of using the same parameters m and p as in the fourth line but with [36]’s method. Their resulting security level $\lambda = 106$ dips below the 128-bit security standard.

Comparison with non-batched alternatives. Up to this point, we have compared the performance of our HTS implementation exclusively to previous best-in-class *batched* implementations of a similar algorithm. [20] is the state-of-the-art alternative for comparison-based *non-batched* HE algorithms. Their solution uses the TFHE encryption scheme and improves upon [15] by designing the fastest homomorphic k -nearest neighbors algorithm in the literature. Extrapolating roughly from the numbers provided in [20], we can (generously) estimate the time needed by their algorithm to sort 4 values of 8 bits to be $> 0.5s$. Given our results in Table 1, the use of such a method can only be preferable to ours in the pathologically small cases where the ML model only has 90 parameters, which is definitely not representative of present-day deep learning.

5 SABLE: Secure And Byzantine robust Learning

In this section, we introduce and explain SABLE. We also present and discuss the acceleration that node subsampling provides.

5.1 Algorithm Description

It is important to note that the instructions below only apply to the honest nodes in the system. By this, we mean that the algorithm asks every node to follow the protocol, but only the honest nodes are guaranteed to correctly perform these operations.

Initially, the server chooses the initial model parameters θ_0 and communicates them to all nodes. Every honest node i thus sets its initial (local) set of parameters $\theta_0^{(i)}$ to θ_0 . In every iteration $t \in \{1, \dots, T\}$ of SABLE, the following operations are executed. First, every honest node i randomly samples a batch of datapoints from its local dataset D_i . On this batch, a stochastic estimate of the gradient is computed using the last model parameters $\theta_{t-1}^{(i)}$, and is referred to as $g_t^{(i)}$. Then, i computes the momentum $m_t^{(i)}$ of the gradient: $m_t^{(i)} = \beta m_{t-1}^{(i)} + (1 - \beta)g_t^{(i)}$, where $m_0^{(i)} = 0$ and $\beta \in (0, 1)$. Before encrypting it, every honest node quantizes the computed momentum to obtain $\tilde{m}_t^{(i)}$. To do so, honest node i first *clamps* $m_t^{(i)}$ using the clamp parameter $C > 0$, thus bringing all the coordinates of the clamped momentum into the range $[-C, C]$. More formally, every coordinate x of $m_t^{(i)}$ is replaced by $\min(\max(x, -C), C)$. The clamped momentum is then multiplied by the quantization parameter $Q = 2^{\delta-1}/C$, where $\delta > 1$ is the bit precision of the algorithm, and rounded to the nearest integer per coordinate. In other words, quantization guarantees that every coordinate of $\tilde{m}_t^{(i)}$ is represented by δ bits. Each honest node i then encrypts $\tilde{m}_t^{(i)}$ and sends the corresponding ciphertext $c_t^{(i)}$ to the server.

Upon receiving all ciphertexts, the server aggregates the submitted vectors using HTS to obtain the encrypted *trimmed sum* C_t , which is then broadcast to all nodes. Every honest node i decrypts C_t to obtain the plaintext $P_t^{(i)}$. As explained in Section 3.4, the plaintext $P_t^{(i)}$ at every honest node i must be divided by the number of summed vectors (i.e., $n - 2f$) to obtain the *trimmed mean* $TM_t^{(i)}$ (see eqs 6-7). Unlike Algorithm 1, the server does not update the model. Indeed, every honest node i locally updates its current estimate of the model parameters $\theta_t^{(i)} = \theta_{t-1}^{(i)} - \gamma TM_t^{(i)}$, where γ is the learning rate. Finally, since the initial model parameters $\theta_0^{(i)}$ and the plaintexts $P_t^{(i)}$ are equal $\forall i$ at every step t , Algorithm 2 outputs the same final model $\theta_T^{(i)}$ for every honest node i .

The case of HMED. Note that in the case of using HMED instead of HTS as aggregation method, the algorithm remains the same for the most part with one exception. The plaintext $P_t^{(i)}$ at every honest node i must not be divided by $n - 2f$ since HMED directly computes the coordinate-wise median. The update rule of the model thus becomes: $\theta_t^{(i)} = \theta_{t-1}^{(i)} - \gamma P_t^{(i)}$.

5.2 Acceleration by Node Subsampling

As mentioned in Section 4, the running time of HTS (and HMED) is quadratic in the number of aggregated ciphertexts. Therefore, having more nodes in the system leads to a considerable increase in the execution time of the homomorphic aggregators. For example, increasing n from 5 to 15 leads to a significant increase of the *amortized* execution time of HTS from 3.17 ms to 30.75 ms ($\sim 10\times$), when using a precision of 4 bits. This quadratic dependency on the number of nodes motivates us to investigate the use of *node subsampling* at the server prior to the aggregation, explained below. In fact, when $2f + 1 < n$ and node subsampling is enabled, the server samples uniformly at random and without replacement $2f + 1$ nodes among n in every step t , and executes HTS only on their corresponding ciphertexts. This enables the server to aggregate fewer vectors, while still guaranteeing the presence of an honest majority among the subsampled nodes. This technique allows us to significantly reduce the computational time of the aggregators and thus tolerate distributed systems of larger size. Furthermore, we note that executing HTS with node subsampling is exactly equivalent to computing HMED on the subsampled ciphertexts. Indeed, (7) returns exactly the coordinate-wise median of the input vectors when $n = 2f + 1$. We present the totality of the described protocol in Algorithm 2.

6 Empirical Evaluation

In this section, we empirically evaluate the performance of SABLE on standard image classification tasks, in a simulated distributed cross-silo system, and in several adversarial scenarios. In Section 6.1, we discuss the experimental setup including the datasets and models used. In Section 6.2, we showcase the empirical performance of SABLE in terms of learning accuracy. Finally, we present the computational cost of HTS (and HMED) in Section 6.3.

⁹*Unif*^(a)(A) denotes the sampling of a elements from the set A uniformly at random and without replacement.

Algorithm 2 SABLE

▷ Initial model $\theta_0 = \theta_0^{(i)}$ for all nodes i , initial momentum $m_0^{(i)} = 0$ for all nodes i , clamp parameter $C > 0$, bit precision $\delta > 1$, learning rate γ , momentum coefficient $\beta \in (0, 1)$, total number of nodes $n > 0$, number of Byzantine nodes $f \geq 0$, Boolean *subsampling*, and number of steps T .

- 1: **for** $t = 1, \dots, T$ **do**
- 2: **Every honest node i does in parallel**
- 3: Compute gradient $g_t^{(i)}$ on $\theta_{t-1}^{(i)}$
- 4: Compute momentum $m_t^{(i)} = \beta m_{t-1}^{(i)} + (1 - \beta)g_t^{(i)}$
- 5: Quantize momentum $\tilde{m}_t^{(i)} = \text{QUA}(m_t^{(i)}, \delta, C)$
- 6: Compute ciphertext $c_t^{(i)} = \text{ENC}(\tilde{m}_t^{(i)})$
- 7: Send $c_t^{(i)}$ to **Server**
- 8: **end block**
- 9: $S_t = \{1, \dots, n\}$
- 10: **if** *subsampling* **then**
- 11: $S_t = \text{Unif}^{(2f+1)}(\{1, \dots, n\})^9$
- 12: **end if**
- 13: **Server** aggregates $C_t = \text{HTS}(\{c_t^{(i)} \mid i \in S_t\})$
- 14: **Server** sends C_t to all nodes
- 15: **Every honest node i does in parallel**
- 16: Decrypt ciphertext $P_t^{(i)} = \text{DEC}(C_t)$
- 17: Compute trimmed mean $TM_t^{(i)} = \frac{1}{|S_t| - 2f} P_t^{(i)}$
- 18: Locally update model $\theta_t^{(i)} = \theta_{t-1}^{(i)} - \gamma TM_t^{(i)}$
- 19: **end block**
- 20: **end for**
- 21: **Every honest node i returns** $\theta_T^{(i)}$

6.1 Experimental Setup

Datasets, preprocessing, and data heterogeneity. In our experiments, we consider three standard image classification datasets, namely MNIST [22], Fashion-MNIST [70], and CIFAR-10 [41]. The input images of MNIST are normalized with mean 0.1307 and standard deviation 0.3081, while the images of Fashion-MNIST are horizontally flipped. Moreover, CIFAR-10 is expanded with horizontally flipped images, along with per channel normalization of means 0.4914, 0.4822, 0.4465, and standard deviations 0.2023, 0.1994, 0.2010. In order to simulate a realistic cross-silo environment where nodes could have different data distributions, we split the datasets across nodes in a heterogeneous fashion. Consequently, we make the different nodes sample from the original datasets using a Dirichlet distribution of parameter α , as proposed in [35]. The smaller the α is, the more heterogeneous the setting is. For MNIST, we set $\alpha = 1$, while for the more challenging Fashion-MNIST dataset, we fix $\alpha = 5$. A pictorial representation of the induced heterogeneity depending on α can be found in Appendix D.1. For CIFAR-10, we consider a homogeneous distribution due to the inherent difficulty of the task, and split the dataset across nodes uniformly at random.

Distributed system and Byzantine regimes. We consider a cross-silo distributed system composed of an honest-but-curious

server and n nodes. We execute SABLE in two settings, namely $n = 15$ for MNIST and Fashion-MNIST and $n = 9$ for CIFAR-10. We test our algorithm in two Byzantine regimes by varying the number of Byzantine nodes present in the system. Specifically, $f \in \{3, 5\}$ on MNIST and Fashion-MNIST, and $f \in \{2, 3\}$ on CIFAR-10.

Models and hyperparameters. On MNIST, we train a feed-forward neural network of 79,510 parameters composed of two fully connected linear layers (model 1); while on Fashion-MNIST a convolutional neural network (CNN) of 431,080 parameters (model 2) is used. On both datasets, we run SABLE for $T = 1,000$ steps, using a batch-size $b = 25$, a fixed learning rate $\gamma = 0.5$ for model 1 and 0.1 for model 2, momentum parameter $\beta = 0.99$, and clamp parameter $C = 0.001$. Moreover, the negative log likelihood loss is used as well as l2-regularization of 10^{-4} . Furthermore, we consider a bit precision of $\delta = 2$ bits and 3 bits on MNIST and Fashion-MNIST, respectively. On the most challenging task, i.e., CIFAR-10, we train an even larger CNN of 712,854 parameters (model 3) for $T = 2,000$ steps, with $b = 50$, $\gamma = 0.5$, $\beta = 0.99$, and $C = 0.004$. We consider a bit precision of $\delta = 4$ bits, and the cross-entropy loss is employed to train model 3. The detailed architectures of the models are presented in Appendix D.2.

Benchmarking and performance evaluation. We evaluate the learning performance of SABLE compared to its non-private counterpart Robust-DSGD (i.e., Algorithm 1 with $F = \text{CWTM}$), and its non-robust counterpart HE-DSGD¹⁰. Our objective is to assess the *security* and *robustness* costs of our algorithm in terms of learning compared to Robust-DSGD and HE-DSGD, respectively. In other words, we are interested in how much the accuracy of the model drops when upgrading Robust-DSGD with security (by quantizing and encrypting momentums) or when granting robustness to HE-DSGD (by replacing homomorphic averaging with HTS). As benchmark, we also compare our algorithm to DSGD. Furthermore, we also run our algorithm when *node subsampling* is enabled and refer to it as *SABLE-SUB*.

Byzantine attacks. In our experiments, the Byzantine nodes execute four state-of-the-art attacks, namely A Little is Enough (ALIE) [7], Fall of Empires (FOE) [72], Labelflipping (LF) [3], and Mimic [39], detailed below. Let \bar{v}_t be the average of the vectors sent by the honest nodes in step t .

- (1) **LF:** Byzantine nodes perform a label flip/rotation by replacing every label l in their datasets by $9 - l$, since the labels of the considered datasets are in $\{0, \dots, 9\}$. Their gradients are thus computed on flipped labels.
- (2) **Mimic:** In heterogeneous settings, Byzantine nodes mimic honest nodes by sending their vectors. We implement the heuristic in [39] to determine the optimal node to mimic in every step t .
- (3) **FOE:** Byzantine nodes send $(1 - \tau)\bar{v}_t$ in step t , where $\tau \in \mathbb{R}$ represents the attack factor. Note that executing FOE with $\tau = 2$ is equivalent to the well-known Signflipping attack [3].
- (4) **ALIE:** Byzantine nodes send $\bar{v}_t + \tau \cdot \sigma_t$ in step t , where σ_t is the coordinate-wise standard deviation of the honest vectors and $\tau \in \mathbb{R}$ represents the attack factor.

In our experiments, we implement optimized versions of ALIE and FOE. The attack factor τ is determined using a greedy algorithm that

¹⁰Equivalent to running DSGD in the encrypted domain using homomorphic averaging.

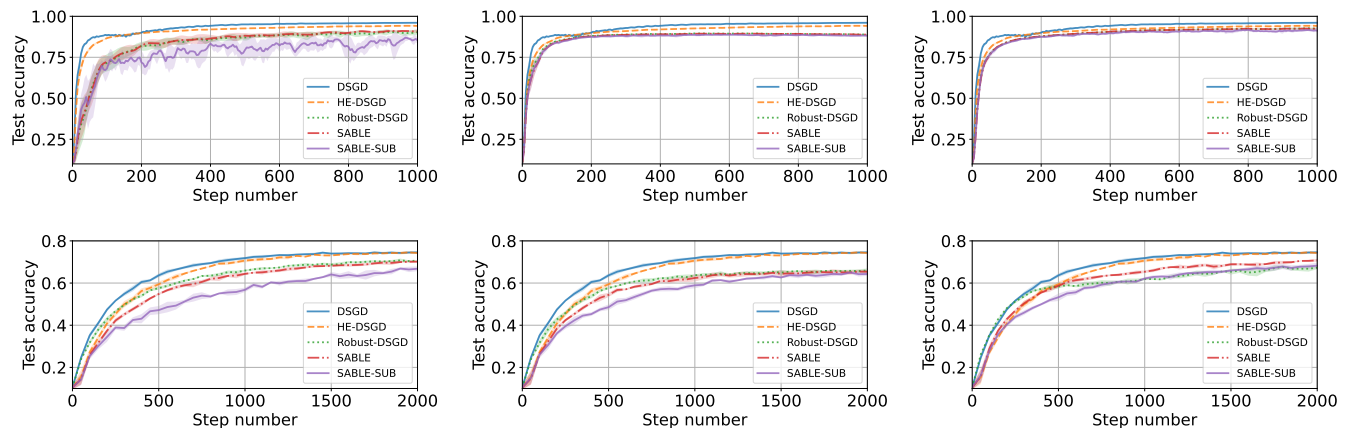


Figure 1: Row 1: MNIST with $f = 5$ and $n = 15$. Row 2: CIFAR-10 with $f = 2$ and $n = 9$. The Byzantine nodes execute the FOE (left), ALIE (center), and LF (right) attacks. The plot for Mimic on MNIST can be found in Appendix F.

performs a linear search over a predefined range of values. In every step t , the optimal τ is determined by choosing the value maximising the L_2 -distance between \bar{v}_t and the output of the aggregation.

Code details. We use the standard Python library for deep learning PyTorch [54] to run all our ML experiments. We execute DSGD and Robust-DSGD using PyTorch’s default 32-bit precision. HE-DSGD is run with the same bit precision as SABLE. The ML experiments are executed using seeds 1 to 5. All FHE times are obtained using the same machine with a 12th Gen Intel® Core™ i7-12700H \times 14 processor and 64GB of RAM. Our code can be found on the private Bitbucket repository <https://bitbucket.org/he-sar-dsgd/workspace/overview/>. To log in, use the username "he.sar.dsgd@gmail.com" with the password "sable-code-popets-2024". We also plan to make the code public upon acceptance.

6.2 ML Performance of SABLE

In this section, we evaluate the performance of SABLE in terms of **learning accuracy**. We consider three datasets of increasing difficulty, namely MNIST, Fashion-MNIST, and CIFAR-10, on which we train three models of increasing complexity. The empirical results on MNIST with $f = 5$ and CIFAR-10 with $f = 2$ are displayed in Figure 1. We present the remaining plots in Appendix F.

MNIST. Our algorithm manifests strong robustness to Byzantine nodes, consistently against four Byzantine attacks and in both Byzantine regimes (refer also to Figures 5 and 6 in Appendix F). In fact, despite using a much smaller bit precision (2 vs 32 bits), SABLE matches the learning performance of its non-private (and full-precision) counterpart Robust-DSGD, without leaking any information to the server. This highlights the practical relevance of our solution, and suggests that its security cost compared to Robust-DSGD is very low in most settings. We also observe that the robustness cost of our algorithm compared to its non-robust counterparts is also negligible. Indeed, as shown in Figure 1, SABLE is able to yield similar accuracies to Byzantine-free HE-DSGD (and even DSGD), while tolerating 5 Byzantine nodes among $n = 15$. It is important to note that the slight difference in the performances of

DSGD and HE-DSGD is only due to the much smaller bit precision $\delta = 2$ used by the latter algorithm. Furthermore, we discuss in Appendix E the importance of appropriately setting the value C of the clamp parameter, and its effect on the performance of SABLE.

Finally, we note that subsampling is a solution that works very well empirically. Indeed, despite taking into account fewer vectors, SABLE-SUB still showcases similar ML performances to the original algorithm while aggregating less ciphertexts.

CIFAR-10. We first notice a larger discrepancy between the performances of SABLE and (HE-)DSGD on CIFAR-10 compared to MNIST. This suggests that the robustness cost of our algorithm is higher in this case, due to the intrinsic difficulty of the task at hand. However, this cost is inevitable in order to be able to successfully tolerate the presence of Byzantine nodes in the system. This observation can also be seen in the difference in the performances of Robust-DSGD and DSGD. However, despite using only $\delta = 4$ bits in SABLE, our algorithm still matches the performance of its full-precision counterpart, namely Robust-DSGD, consistently against all three Byzantine attacks. This highlights the low security cost of our solution resulting from the encryption of gradients, and confirms the relevance of SABLE in practical systems. Finally, node subsampling is also very effective in this setting. Figure 1 also shows that SABLE-SUB matches the original algorithm.

6.3 HTS Execution Times

In this section, we evaluate the execution time of HTS in the experimental settings presented in Section 6.1. We study the computational performance of HTS in two instantiations of SABLE: one where subsampling is not used (Table 2), and one where node subsampling is enabled (Table 3).

We also consider four different hardware models for the server. In fact, we quantify the computational power of the server using the number of cores available to be used concurrently. Indeed, we consider (1) a *lightweight* machine with 1 core, (2) a *moderate* machine with 16 cores, a *powerful* machine with 32 cores, and finally (4) a *high end* machine with 64 cores. As previously mentioned, since HTS is a coordinate-wise operator, the different cores can

be used in parallel to execute HTS on separate blocks of coordinates independently, thus accelerating the computations. In all our experiments, we guarantee at least an FHE security level $\lambda \geq 128$.

Dataset	Model size	δ (bits)	n	Cores	Time	BW
MNIST	79,510	2	15	1	17.34	5
				≥ 16	1.24	
Fashion	431,080	3	15	1	145.13	27
				16	9.68	
				32	5.81	
				64	3.87	
CIFAR	712,854	4	9	1	125.16	88
				16	8.07	
				32	4.04	
				64	2.02	

Table 2: Aggregation time without node subsampling. This table presents the time (in minutes) needed for one evaluation of HTS over n ciphertexts. We also present the total bandwidth (BW) in KBytes needed per node in one iteration (i.e., sending the encrypted gradient and receiving the result). We guarantee $\lambda \geq 128$ (also for Table 3).

More cores, less time ... As expected, Table 2 shows that using more powerful machines directly translates into lower execution times. Indeed, the time required by 1 core to execute HTS on $n = 15$ ciphertexts on MNIST is 17.34 minutes. This time is considerably reduced by a factor of ~ 14 to reach 1.24 minutes, when at least 16 cores are used instead. Note that these practical execution times are also imputable to the lower precisions considered ($\delta = 2, 3, 4$ bits, depending of the dataset). As discussed in Section 6.2, despite this decrease in precision, SABLE still matches the ML performance of its full-precision counterpart Robust-DSGD. Moreover, we can observe that more complex learning tasks typically need more powerful machines in order to compute HTS. Indeed, Table 2 shows that a 16-core machine is required in order to efficiently perform HTS on MNIST in 1.24 minutes. On Fashion-MNIST, a *powerful* server machine with at least 32 cores is needed in order to obtain a feasible time (5.81 minutes); given that $n = 15$ and the model trained has 431,080 parameters. Finally, on CIFAR-10, despite the smaller number of nodes considered, the challenging nature of the task (i.e., the very large size of the model) requires 32 cores to guarantee a reasonable time below 5 minutes. A *high end* machine with 64 cores halves that time to obtain 2.02 minutes.

... up to a certain point. As indicated by the lines for MNIST in Table 2, there is a point beyond which adding more cores no longer decreases the aggregation time. The reason is the following. There is a base homomorphic computation that is done over data encrypted into one ciphertext. If the model size is large enough, more than one ciphertext is needed, and we can then parallelize trivially over those additional ciphertexts. Therefore, our gains stop when the number of cores reaches the number of ciphertexts used.

Subsampling significantly decreases the computational cost. If the server is limited in computational power, node subsampling provides an interesting solution as it significantly accelerates

Dataset	Model size	f	Cores	Time	Acc. (\times)			
MNIST	79,510	3	1	2.61	6.64			
			16	0.29	4.28			
			≥ 32	0.14	8.86			
		5	1	9.15	1.90			
			16	0.65	1.91			
			≥ 32	0.65	1.91			
Fashion	431,080	3	1	29.48	4.92			
			16	1.97	4.91			
			32	1.18	4.92			
			64	0.79	4.90			
		5	1	79.94	1.82			
			16	5.33	1.82			
			32	3.20	1.82			
			64	2.13	1.82			
			CIFAR	712,854	2	1	37.84	3.31
						16	2.38	3.39
32	1.30	3.11						
64	0.65	3.11						
3	1	83.57			1.50			
	16	5.39			1.50			
	32	2.70			1.50			
	64	1.35			1.50			

Table 3: Aggregation time with node subsampling. This table presents the time (in minutes) needed for one evaluation of HTS over $2f + 1$ ciphertexts. The acceleration "Acc." with respect to Table 2 (no subsampling) is also reported.

HTS on all three learning tasks. Looking at Table 2, we can see that using a 64-core machine is the only practically relevant alternative to train a model of 712,854 parameters on CIFAR-10. The corresponding execution time is 2.02 minutes. Downgrading the server directly leads to an increase in the computational time by factors of $\sim 2, 4,$ and 64 when using 32, 16, and 1 cores, respectively. Interestingly, node subsampling enables HTS to reach almost the same computational performance using fourth and half of the resources when $f = 2$ and 3 , respectively. Indeed, 16 cores are able to reach 2.38 minutes per aggregation when $f = 2$, and 32 cores are enough to obtain 2.70 minutes when $f = 3$. Contrastingly, 64 cores are required to break the 2 minute mark without node subsampling (Table 2). Furthermore, applying node subsampling on 64 cores leads to a time acceleration of $3.11\times$ and $1.50\times$ when $f = 2$ and 3 , respectively. The same analysis is also applicable for the two remaining datasets. Moreover, an interesting observation on MNIST is that without subsampling, the time for one homomorphic aggregation using only 1 core is 17.34 minutes, which is really impractical. However, node subsampling decreases the aggregation time by $6.64\times$ when $f = 3$, resulting in the very reasonable 2.61 minutes using only 1 core. This highlights again the practicality of node subsampling by allowing us to employ cheaper server machines when performing expensive homomorphic aggregations.

HMED execution times. As described in Section 4.3, HMED is computed as a specific sub-case of HTS. When evaluating the performance of HMED, we find no discernible difference with the

timings presented in Tables 2 and 3. Since HMed boils down to using a different polynomial evaluation at the last step of HTS, no additional cost is incurred.

7 Concluding Remarks

In this work, we present SABLE, a building-block for extending Robust-DSGD with training data confidentiality guarantees by means of HE. SABLE is robust against Byzantine nodes, achieves state-of-the-art cryptographic security, and protects the data privacy of the nodes from the server. At the core of SABLE lies our main contribution, namely HTS, our novel homomorphic operator for the robust aggregator CWTM [73]. To develop HTS, we propose a new plaintext encoding method that accelerates state-of-the-art homomorphic sorting. Most importantly, HTS would have been more challenging to implement efficiently without this contribution. An additional by-product of our work is the ability to also implement HMed, a homomorphic operator for CWMED [73], without incurring additional costs.

REFERENCES

- [1] Martin Albrecht, Melissa Chase, Hao Chen, Jintai Ding, Shafi Goldwasser, Sergey Gorbunov, Shai Halevi, Jeffrey Hoffstein, Kim Laine, Kristin Lauter, Satya Lokam, Daniele Micciancio, Dustin Moody, Travis Morrison, Amit Sahai, and Vinod Vaikuntanathan. 2018. *Homomorphic Encryption Security Standard*. Technical Report. HomomorphicEncryption.org, Toronto, Canada.
- [2] Martin R. Albrecht, Rachel Player, and Sam Scott. 2015. On the concrete hardness of Learning with Errors. *Journal of Mathematical Cryptology* 9, 3 (2015), 169–203. <https://doi.org/10.1515/jmc-2015-0016>
- [3] Zeyuan Allen-Zhu, Faeze EbrahimiGhazani, Jerry Li, and Dan Alistarh. 2020. Byzantine-Resilient Non-Convex Stochastic Gradient Descent. In *International Conference on Learning Representations*.
- [4] Youssef Allouah, Sadegh Farhadkhani, Rachid Guerraoui, Nirupam Gupta, Rafael Pinot, and John Stephan. 2023. Fixing by Mixing: A Recipe for Optimal Byzantine ML under Heterogeneity. In *Proceedings of The 26th International Conference on Artificial Intelligence and Statistics (Proceedings of Machine Learning Research, Vol. 206)*, Francisco Ruiz, Jennifer Dy, and Jan-Willem van de Meent (Eds.). PMLR, 1232–1300. <https://proceedings.mlr.press/v206/allouah23a.html>
- [5] Youssef Allouah, Rachid Guerraoui, Nirupam Gupta, Rafael Pinot, and John Stephan. 2023. On the Privacy-Robustness-Utility Trilemma in Distributed Learning. In *Proceedings of the 40th International Conference on Machine Learning (Proceedings of Machine Learning Research, Vol. 202)*, Andreas Krause, Emma Brunskill, Kyunghyun Cho, Barbara Engelhardt, Sivan Sabato, and Jonathan Scarlett (Eds.). PMLR, 569–626. <https://proceedings.mlr.press/v202/allouah23a.html>
- [6] Ahmad Al Badawi, Jack Bates, Flavio Bergamaschi, David Bruce Cousins, Saroja Erabelli, Nicholas Genise, Shai Halevi, Hamish Hunt, Andrey Kim, Yongwoo Lee, Zeyu Liu, Daniele Micciancio, Ian Quah, Yuriy Polyakov, Saraswathy R.V., Kurt Rohloff, Jonathan Saylor, Dmitriy Suponitsky, Matthew Triplett, Vinod Vaikuntanathan, and Vincent Zucca. 2022. OpenFHE: Open-Source Fully Homomorphic Encryption Library. *Cryptology ePrint Archive*, Paper 2022/915. <https://eprint.iacr.org/2022/915> <https://eprint.iacr.org/2022/915>
- [7] Moran Baruch, Gilad Baruch, and Yoav Goldberg. 2019. A Little Is Enough: Circumventing Defenses For Distributed Learning. In *Advances in Neural Information Processing Systems 32: Annual Conference on Neural Information Processing Systems 2019, 8-14 December 2019, Long Beach, CA, USA*.
- [8] Dimitri Bertsekas and John Tsitsiklis. 2015. *Parallel and distributed computation: numerical methods*. Athena Scientific.
- [9] Peva Blanchard, El Mahdi El Mhamdi, Rachid Guerraoui, and Julien Stainer. 2017. Machine Learning with Adversaries: Byzantine Tolerant Gradient Descent. In *Advances in Neural Information Processing Systems 30*, I. Guyon, U. V. Luxburg, S. Bengio, H. Wallach, R. Fergus, S. Vishwanathan, and R. Garnett (Eds.). Curran Associates, Inc., 119–129.
- [10] Keith Bonawitz, Vladimir Ivanov, Ben Kreuter, Antonio Marcedone, H. Brendan McMahan, Sarvar Patel, Daniel Ramage, Aaron Segal, and Karn Seth. 2017. Practical Secure Aggregation for Privacy-Preserving Machine Learning. In *Proceedings of the 2017 ACM SIGSAC Conference on Computer and Communications Security (Dallas, Texas, USA) (CCS '17)*. Association for Computing Machinery, New York, NY, USA, 1175–1191. <https://doi.org/10.1145/3133956.3133982>
- [11] Zvika Brakerski. 2012. *Fully Homomorphic Encryption without Modulus Switching from Classical GapSVP*. Lecture Notes in Computer Science, Vol. 7417. Springer Berlin Heidelberg, Berlin, Heidelberg, 868–886. https://doi.org/10.1007/978-3-642-32009-5_50
- [12] Zvika Brakerski, Craig Gentry, and Vinod Vaikuntanathan. 2011. Fully Homomorphic Encryption without Bootstrapping. *Electron. Colloquium Comput. Complex.* 18 (2011), 111. <http://dblp.uni-trier.de/db/journals/eccc/eccc18.html#BrakerskiGV11>
- [13] Xiaoyu Cao, Minghong Fang, Jia Liu, and Neil Zhenqiang Gong. 2021. FLTrust: Byzantine-robust Federated Learning via Trust Bootstrapping. In *28th Annual Network and Distributed System Security Symposium, NDSS 2021, virtually, February 21-25, 2021*. The Internet Society. <https://www.ndss-symposium.org/ndss-paper/fltrust-byzantine-robust-federated-learning-via-trust-bootstrapping/>
- [14] Gizem S. Çetin, Yarkın Doröz, Berk Sunar, and Erkan Savaş. 2015. Depth Optimized Efficient Homomorphic Sorting. In *Proceedings of the 4th International Conference on Progress in Cryptology – LATINCRYPT 2015 - Volume 9230*. Springer-Verlag, Berlin, Heidelberg, 61–80. https://doi.org/10.1007/978-3-319-22174-8_4
- [15] Olive Chakraborty and Martin Zuber. 2022. Efficient and Accurate Homomorphic Comparisons. In *Proceedings of the 10th Workshop on Encrypted Computing & Applied Homomorphic Cryptography (Los Angeles, CA, USA) (WAHC'22)*. Association for Computing Machinery, New York, NY, USA, 35–46. <https://doi.org/10.1145/3560827.3563375>
- [16] Yudong Chen, Lili Su, and Jiaming Xu. 2017. Distributed statistical machine learning in adversarial settings: Byzantine gradient descent. *Proceedings of the ACM on Measurement and Analysis of Computing Systems* 1, 2 (2017), 1–25.
- [17] Yudong Chen, Lili Su, and Jiaming Xu. 2017. Distributed statistical machine learning in adversarial settings: Byzantine gradient descent. *Proceedings of the ACM on Measurement and Analysis of Computing Systems* 1, 2 (2017), 1–25.
- [18] Jung Hee Cheon, Andrey Kim, Miran Kim, and Yongsoo Song. 2017. Homomorphic Encryption for Arithmetic of Approximate Numbers. In *Advances in Cryptology – ASIACRYPT 2017*, Tsuyoshi Takagi and Thomas Peyrin (Eds.). Springer International Publishing, Cham, 409–437.
- [19] Ilaria Chillotti, Nicolas Gama, Mariya Georgieva, and Malika Izabachène. 2020. TFHE: Fast Fully Homomorphic Encryption Over the Torus. *J. Cryptol.* 33, 1 (jan 2020), 34–91. <https://doi.org/10.1007/s00145-019-09319-x>
- [20] Kelong Cong, Robin Geelen, Jiayi Kang, and Jeongeun Park. 2023. Efficient and Secure k -NN Classification from Improved Data-Oblivious Programs and Homomorphic Encryption. *Cryptology ePrint Archive* (2023).
- [21] Henry Corrigan-Gibbs and Dan Boneh. 2017. Prio: Private, Robust, and Scalable Computation of Aggregate Statistics. In *14th USENIX Symposium on Networked Systems Design and Implementation (NSDI 17)*. USENIX Association, Boston, MA, 259–282. <https://www.usenix.org/conference/nsdi17/technical-sessions/presentation/corrigan-gibbs>
- [22] Li Deng. 2012. The mnist database of handwritten digit images for machine learning research. *IEEE Signal Processing Magazine* 29, 6 (2012), 141–142.
- [23] El Mahdi El Mhamdi, Rachid Guerraoui, and Sébastien Rouault. 2018. The Hidden Vulnerability of Distributed Learning in Byzantium. In *Proceedings of the 35th International Conference on Machine Learning (Proceedings of Machine Learning Research, Vol. 80)*, Jennifer Dy and Andreas Krause (Eds.). PMLR, 3521–3530. <https://proceedings.mlr.press/v80/mhamdi18a.html>
- [24] El Mahdi El Mhamdi, Rachid Guerraoui, and Sébastien Rouault. 2021. Distributed Momentum for Byzantine-resilient Stochastic Gradient Descent. In *9th International Conference on Learning Representations, ICLR 2021, Vienna, Austria, May 4–8, 2021*. OpenReview.net.
- [25] Junfeng Fan and Frederik Vercauteren. 2012. Somewhat Practical Fully Homomorphic Encryption. (2012). <https://eprint.iacr.org/2012/144> Report Number: 144.
- [26] Sadegh Farhadkhani, Rachid Guerraoui, Nirupam Gupta, Rafael Pinot, and John Stephan. 2022. Byzantine Machine Learning Made Easy By Resilient Averaging of Momentums. In *Proceedings of the 39th International Conference on Machine Learning (Proceedings of Machine Learning Research, Vol. 162)*, Kamalika Chaudhuri, Stefanie Jegelka, Le Song, Csaba Szepesvari, Gang Niu, and Sivan Sabato (Eds.). PMLR, 6246–6283.
- [27] Jonas Geiping, Hartmut Bauermeister, Hannah Dröge, and Michael Moeller. 2020. Inverting Gradients - How easy is it to break privacy in federated learning?. In *Advances in Neural Information Processing Systems*, H. Larochelle, M. Ranzato, R. Hadsell, M.F. Balcan, and H. Lin (Eds.), Vol. 33. Curran Associates, Inc., 16937–16947. https://proceedings.neurips.cc/paper_files/paper/2020/file/c4ede56bb98819ae6112b20ac6bf145-Paper.pdf
- [28] Quan Geng, Wei Ding, Ruiqi Guo, and Sanjiv Kumar. 2020. Tight Analysis of Privacy and Utility Tradeoff in Approximate Differential Privacy. In *Proceedings of the Twenty Third International Conference on Artificial Intelligence and Statistics (Proceedings of Machine Learning Research, Vol. 108)*, Silvia Chiappa and Roberto Calandra (Eds.). PMLR, 89–99. <https://proceedings.mlr.press/v108/geng20a.html>
- [29] Ran Gilad-Bachrach, Nathan Dowlin, Kim Laine, Kristin Lauter, Michael Naehrig, and John Wernsing. 2016. CryptoNets: Applying Neural Networks to Encrypted Data with High Throughput and Accuracy. In *Proceedings of The 33rd International Conference on Machine Learning (Proceedings of Machine Learning Research, Vol. 48)*, Maria Florina Balcan and Kilian Q. Weinberger (Eds.). PMLR, New York, New York, USA, 201–210. <https://proceedings.mlr.press/v48/gilad>

- bachrach16.html
- [30] Rachid Guerraoui, Nirupam Gupta, Rafaël Pinot, Sébastien Rouault, and John Stephan. 2021. Differential Privacy and Byzantine Resilience in SGD: Do They Add Up?. In *Proceedings of the 2021 ACM Symposium on Principles of Distributed Computing* (Virtual Event, Italy) (PODC'21). Association for Computing Machinery, New York, NY, USA, 391–401. <https://doi.org/10.1145/3465084.3467919>
- [31] Nirupam Gupta and Nitin H Vaidya. 2020. Fault-tolerance in distributed optimization: The case of redundancy. In *Proceedings of the 39th Symposium on Principles of Distributed Computing*. 365–374.
- [32] Shai Halevi and Victor Shoup. 2020. Design and implementation of HELib: a homomorphic encryption library. Cryptology ePrint Archive, Paper 2020/1481. <https://eprint.iacr.org/2020/1481>
- [33] Meng Hao, Hongwei Li, Guowen Xu, Hanxiao Chen, and Tianwei Zhang. 2021. Efficient, Private and Robust Federated Learning. In *Annual Computer Security Applications Conference* (Virtual Event, USA) (ACSAC '21). Association for Computing Machinery, New York, NY, USA, 45–60. <https://doi.org/10.1145/3485832.3488014>
- [34] Lie He, Sai Praneeth Karimireddy, and Martin Jaggi. 2020. Secure Byzantine-Robust Machine Learning. arXiv:2006.04747 [cs.LG]
- [35] Tzu-Ming Harry Hsu, Hang Qi, and Matthew Brown. 2019. Measuring the Effects of Non-Identical Data Distribution for Federated Visual Classification. <https://doi.org/10.48550/ARXIV.1909.06335>
- [36] Iliia Iliashenko and Vincent Zucca. 2021. Faster homomorphic comparison operations for BGV and BFV. *Proceedings on Privacy Enhancing Technologies* 2021 (07 2021), 246–264. <https://doi.org/10.2478/popets-2021-0046>
- [37] Chiraag Juvekar, Vinod Vaikuntanathan, and Anantha Chandrakasan. 2018. GAZELLE: A Low Latency Framework for Secure Neural Network Inference. In *Proceedings of the 27th USENIX Conference on Security Symposium* (Baltimore, MD, USA) (SEC'18). USENIX Association, USA, 1651–1668.
- [38] Sai Praneeth Karimireddy, Lie He, and Martin Jaggi. 2021. Learning from History for Byzantine Robust Optimization. *International Conference On Machine Learning, Vol 139* 139 (2021).
- [39] Sai Praneeth Karimireddy, Lie He, and Martin Jaggi. 2022. Byzantine-Robust Learning on Heterogeneous Datasets via Bucketing. In *International Conference on Learning Representations*. <https://openreview.net/forum?id=jXKKDEi5vJt>
- [40] Yousef Khazbak, Tianxiang Tan, and Guohong Cao. 2020. MLGuard: Mitigating Poisoning Attacks in Privacy Preserving Distributed Collaborative Learning. *2020 29th International Conference on Computer Communications and Networks (ICCCN)* (2020), 1–9. <https://api.semanticscholar.org/CorpusID:218594342>
- [41] Alex Krizhevsky, Vinod Nair, and Geoffrey Hinton. 2014. The CIFAR-10 dataset. *online: http://www.cs.toronto.edu/kriz/cifar.html* 55, 5 (2014).
- [42] Leslie Lamport, Robert Shostak, and Marshall Pease. 1982. The Byzantine Generals Problem. *ACM Trans. Program. Lang. Syst.* 4, 3 (jul 1982), 382–401. <https://doi.org/10.1145/357172.357176>
- [43] Liping Li, Wei Xu, Tianyi Chen, Georgios B. Giannakis, and Qing Ling. 2019. RSA: Byzantine-Robust Stochastic Aggregation Methods for Distributed Learning from Heterogeneous Datasets. *Proceedings of the AAAI Conference on Artificial Intelligence* 33, 01 (Jul. 2019), 1544–1551. <https://doi.org/10.1609/aaai.v33i01.33011544>
- [44] Shuo Liu, Nirupam Gupta, and Nitin H. Vaidya. 2021. Approximate Byzantine Fault-Tolerance in Distributed Optimization. In *Proceedings of the 2021 ACM Symposium on Principles of Distributed Computing* (Virtual Event, Italy) (PODC'21). Association for Computing Machinery, New York, NY, USA, 379–389. <https://doi.org/10.1145/3465084.3467902>
- [45] Qian Lou, Bo Feng, Geoffrey Charles Fox, and Lei Jiang. 2020. Glyph: Fast and Accurately Training Deep Neural Networks on Encrypted Data. In *Advances in Neural Information Processing Systems*, H. Larochelle, M. Ranzato, R. Hadsell, M.F. Balcan, and H. Lin (Eds.), Vol. 33. Curran Associates, Inc., 9193–9202. https://proceedings.neurips.cc/paper_files/paper/2020/file/685ac8cad1be5ac98da9556bc1c8d9e-Paper.pdf
- [46] Jing Ma, Si-Ahmed Naas, Stephan Sigg, and Xixiang Lyu. 2022. Privacy-preserving federated learning based on multi-key homomorphic encryption. *International Journal of Intelligent Systems* 37, 9 (2022), 5880–5901. <https://doi.org/10.1002/int.22818> arXiv:https://onlinelibrary.wiley.com/doi/pdf/10.1002/int.22818
- [47] Xu Ma, Yuqing Zhou, Laihua Wang, and Meixia Miao. 2022. Privacy-preserving Byzantine-robust federated learning. *Computer Standards & Interfaces* 80 (2022), 103561. <https://doi.org/10.1016/j.csi.2021.103561>
- [48] Abbas Madi, Oana Stan, Aurélien Mayoue, Arnaud Grivet-Sébert, Cédric Gouy-Pailler, and Renaud Sirdey. 2021. A Secure Federated Learning framework using Homomorphic Encryption and Verifiable Computing. In *2021 Reconciling Data Analytics, Automation, Privacy, and Security: A Big Data Challenge (RDAAPS)*. 1–8. <https://doi.org/10.1109/RDAAPS48126.2021.9452005>
- [49] Yinbin Miao, Ziteng Liu, Hongwei Li, Kim-Kwang Raymond Choo, and Robert H. Deng. 2022. Privacy-Preserving Byzantine-Robust Federated Learning via Blockchain Systems. *IEEE Transactions on Information Forensics and Security* 17 (2022), 2848–2861. <https://doi.org/10.1109/TIFS.2022.3196274>
- [50] Arup Mondal, Yash More, Ruthu Hulikal Rooparagunath, and Debayan Gupta. 2021. Poster: FLATEE: Federated Learning Across Trusted Execution Environments. In *2021 IEEE European Symposium on Security and Privacy (EuroS&P)* 707–709. <https://doi.org/10.1109/EuroS&P51992.2021.00054>
- [51] Harika Narumanchi, Dishant Goyal, Nitesh Emmadi, and Praveen Gauravaram. 2017. Performance Analysis of Sorting of FHE Data: Integer-Wise Comparison vs Bit-Wise Comparison. In *31st IEEE International Conference on Advanced Information Networking and Applications, AINA 2017, Taipei, Taiwan, March 27-29, 2017*, Leonard Barolli, Makoto Takizawa, Tomoya Enokido, Hui-Huang Hsu, and Chi-Yi Lin (Eds.). IEEE Computer Society, 902–908. <https://doi.org/10.1109/AINA.2017.85>
- [52] Lucien K. L. Ng and Sherman S. M. Chow. 2023. SoK: Cryptographic Neural-Network Computation. In *44th IEEE Symposium on Security and Privacy, SP 2023, San Francisco, CA, USA, 22-25 May 2023*. IEEE Computer Society, 497–514. <https://doi.org/10.1109/SP46215.2023.00198>
- [53] Thien Nguyen, Phillip Rieger, Hossein Yalame, Helen Möllering, Hossein Ferdouzi, Samuel Marchal, Markus Miettinen, Azalia Mirhoseini, Ahmad-Reza Sadeghi, Thomas Schneider, and Shaza Zeitouni. 2021. FLGUARD: Secure and Private Federated Learning. (01 2021).
- [54] Adam Paszke, Sam Gross, Francisco Massa, Adam Lerer, James Bradbury, Gregory Chanan, Trevor Killeen, Zeming Lin, Natalia Gimelshein, Luca Antiga, Alban Desmaison, Andreas Kopf, Edward Yang, Zachary DeVito, Martin Raison, Alykhan Tejani, Sasank Chilamkurthy, Benoit Steiner, Lu Fang, Junjie Bai, and Soumith Chintala. 2019. PyTorch: An Imperative Style, High-Performance Deep Learning Library. In *Advances in Neural Information Processing Systems* 32. Curran Associates, Inc., 8024–8035. <http://papers.neurips.cc/paper/9015-pytorch-an-imperative-style-high-performance-deep-learning-library.pdf>
- [55] Le Trieu Phong, Yoshinori Aono, Takuya Hayashi, Lihua Wang, and Shihoh Moriai. 2018. Privacy-Preserving Deep Learning via Additively Homomorphic Encryption. *IEEE Transactions on Information Forensics and Security* 13, 5 (2018), 1333–1345. <https://doi.org/10.1109/TIFS.2017.2787987>
- [56] Krishna Pillutla, Sham M. Kakade, and Zaid Harchaoui. 2022. Robust Aggregation for Federated Learning. *IEEE Transactions on Signal Processing* 70 (2022), 1142–1154. <https://doi.org/10.1109/TSP.2022.3153135>
- [57] John M. Pollard. 1971. The fast Fourier transform in a finite field. *Math. Comp.* 25 (1971), 365–374.
- [58] Boris T Polyak. 1964. Some methods of speeding up the convergence of iteration methods. *USSR computational mathematics and mathematical physics* 4, 5 (1964), 1–17.
- [59] Yogachandran Rahulamathavan, Charuka Herath, Xiaolan Liu, Sangarapillai Lambotharan, and Carsten Maple. 2023. FHEFL: Fully Homomorphic Encryption Friendly Privacy-Preserving Federated Learning with Byzantine Users. *arXiv preprint arXiv:2306.05112* (2023).
- [60] SEAL 2023. Microsoft SEAL (release 4.1). <https://github.com/Microsoft/SEAL>. Microsoft Research, Redmond, WA..
- [61] Arnaud Grivet Sébert, Rafaël Pinot, Martin Zuber, Cédric Gouy-Pailler, and Renaud Sirdey. 2021. SPEED: secure, PrivateE, and efficient deep learning. *Machine Learning* 110, 4 (mar 2021), 675–694. <https://doi.org/10.1007/s10994-021-05970-3>
- [62] Hayim Shaul, Dan Feldman, and Daniela Rus. 2020. Secure k-ish Nearest Neighbors Classifier. *Proc. Priv. Enhancing Technol.* 2020, 3 (2020), 42–61. <https://doi.org/10.2478/popets-2020-0045>
- [63] Jinhyun So, Basak Guler, and A. Salman Avestimehr. 2020. Byzantine-Resilient Secure Federated Learning. <https://doi.org/10.48550/ARXIV.2007.11115>
- [64] Oana Stan, Vincent Thouvenot, Aymen Boudguiga, Katarzyna Kapusta, Martin Zuber, and Renaud Sirdey. 2022. A Secure Federated Learning: Analysis of Different Cryptographic Tools.
- [65] Arnaud Grivet Sébert, Renaud Sirdey, Oana Stan, and Cédric Gouy-Pailler. 2023. Combining homomorphic encryption and differential privacy in federated learning. In *Proceedings of the 20th Annual International Conference on Privacy, Security & Trust*.
- [66] Benjamin Hong Meng Tan, Hyung Tae Lee, Huaxiong Wang, Shuqin Ren, and Khin Mi Mi Aung. 2021. Efficient Private Comparison Queries Over Encrypted Databases Using Fully Homomorphic Encryption With Finite Fields. *IEEE Transactions on Dependable and Secure Computing* 18, 6 (2021), 2861–2874. <https://doi.org/10.1109/TDSC.2020.2967740>
- [67] Stacey Truex, Nathalie Baracaldo, Ali Anwar, Thomas Steinke, Heiko Ludwig, Rui Zhang, and Yi Zhou. 2019. A Hybrid Approach to Privacy-Preserving Federated Learning. In *Proceedings of the 12th ACM Workshop on Artificial Intelligence and Security* (London, United Kingdom) (AISeC'19). Association for Computing Machinery, New York, NY, USA, 1–11. <https://doi.org/10.1145/3338501.3357370>
- [68] Raj Kirti Velicheti, Derek Xia, and Oluwasanmi Koyejo. 2021. Secure Byzantine-Robust Distributed Learning via Clustering. arXiv:2110.02940 [cs.CR]
- [69] Naiyu Wang, Wenti Yang, Zhitao Guan, Xiaojiang Du, and Mohsen Guizani. 2021. BPDF: A Blockchain Based Privacy-Preserving Federated Learning Scheme. In *2021 IEEE Global Communications Conference (GLOBECOM)*. 1–6. <https://doi.org/10.1109/GLOBECOM46510.2021.9685821>
- [70] Han Xiao, Kashif Rasul, and Roland Vollgraf. 2017. Fashion-MNIST: a Novel Image Dataset for Benchmarking Machine Learning Algorithms. *arXiv preprint arXiv:1708.07747* (2017).
- [71] Cong Xie, Oluwasanmi Koyejo, and Indranil Gupta. 2018. Generalized Byzantine-tolerant SGD. arXiv:1802.10116 [cs.DC]

- [72] Cong Xie, Oluwasanmi Koyejo, and Indranil Gupta. 2019. Fall of Empires: Breaking Byzantine-tolerant SGD by Inner Product Manipulation. In *Proceedings of the Thirty-Fifth Conference on Uncertainty in Artificial Intelligence, UAI 2019, Tel Aviv, Israel, July 22-25, 2019*. 83.
- [73] Dong Yin, Yudong Chen, Ramchandran Kannan, and Peter Bartlett. 2018. Byzantine-robust distributed learning: Towards optimal statistical rates. In *International Conference on Machine Learning*. PMLR, 5650–5659.
- [74] Chengliang Zhang, Suyi Li, Junzhe Xia, Wei Wang, Feng Yan, and Yang Liu. 2020. BatchCrypt: Efficient Homomorphic Encryption for Cross-Silo Federated Learning. In *2020 USENIX Annual Technical Conference (USENIX ATC 20)*. USENIX Association, 493–506. <https://www.usenix.org/conference/atc20/presentation/zhang-chengliang>
- [75] Zhuangzhuang Zhang, Libing Wu, Chuanguo Ma, Jianxin Li, Jing Wang, Qian Wang, and Shui Yu. 2023. LSFL: A Lightweight and Secure Federated Learning Scheme for Edge Computing. *IEEE Transactions on Information Forensics and Security* 18 (2023), 365–379. <https://doi.org/10.1109/TIFS.2022.3221899>
- [76] Bo Zhao, Konda Reddy Mopuri, and Hakan Bilen. 2020. idlg: Improved deep leakage from gradients. *arXiv preprint arXiv:2001.02610* (2020).
- [77] L. Zhao, J. Jiang, B. Feng, Q. Wang, C. Shen, and Q. Li. 2022. SEAR: Secure and Efficient Aggregation for Byzantine-Robust Federated Learning. *IEEE Transactions on Dependable and Secure Computing* 19, 05 (sep 2022), 3329–3342. <https://doi.org/10.1109/TDSC.2021.3093711>
- [78] Heng Zhu and Qing Ling. 2022. Bridging Differential Privacy and Byzantine-Robustness via Model Aggregation. *arXiv:2205.00107* [cs.LG]
- [79] Ligeng Zhu, Zhijian Liu, and Song Han. 2019. Deep Leakage from Gradients. In *Advances in Neural Information Processing Systems*, H. Wallach, H. Larochelle, A. Beygelzimer, F. d’Alché-Buc, E. Fox, and R. Garnett (Eds.), Vol. 32. Curran Associates, Inc. https://proceedings.neurips.cc/paper_files/paper/2019/file/60a6c4002cc7b29142def8871531281a-Paper.pdf
- [80] Martin Zuber and Renaud Sirdey. 2021. Efficient homomorphic evaluation of k-NN classifiers. *Proc. Priv. Enhancing Technol.* 2021, 2 (2021), 111–129.

A Table of notations

n	\triangleq	Number of nodes
f	\triangleq	Number of Byzantine nodes
d	\triangleq	Size of model/gradients
T	\triangleq	Number of steps of SABLE
$g_t^{(i)}$	\triangleq	Gradient of node i at step t
$m_t^{(i)}$	\triangleq	Momentum of node i at step t
$c_t^{(i)}$	\triangleq	Ciphertext of node i at step t
$\theta_t^{(i)}$	\triangleq	Model parameters of node i at step t
γ	\triangleq	Learning rate
β	\triangleq	Momentum coefficient
δ	\triangleq	Bit precision
C	\triangleq	Clamp parameter
m	\triangleq	Index of cyclotomic polynomial
p	\triangleq	Plaintext modulus
q	\triangleq	Ciphertext modulus
λ	\triangleq	Cryptographic security (in bits)
B	\triangleq	Arithmetic base
N	\triangleq	Length of digit decomposition

Table 4: Table of notations used in this paper

B FHE-compliance of Byzantine Aggregators (Full Version)

In this section, we qualitatively review six prominent Byzantine aggregators with respect to their compliance with the mainstream FHE cryptosystems in terms of evaluation cost. We classify these operators into two categories. First, we have geometric approaches which select one or more vectors based on a global criterion, but which are subject to a selection bottleneck in high dimensions. Second, coordinate-wise approaches, which manipulate each coordinate independently, appear to be the most promising, in particular those with a static selection criterion. We base our analysis on the characteristics of the mainstream FHE schemes discussed in Section 3.2, which we use as a yardstick to determine the feasibility of each of these methods.

B.1 Geometric Aggregators

Geometric aggregators generally require the calculation of criteria (e.g., norms, distances) over the nodes’ vectors, which then have to be compared to select one or more vectors. Furthermore, they usually require several levels of comparisons, min/max and argmin/max operators, etc. As such, geometric methods should be better handled by the TFHE cryptosystem. However, since TFHE does not support batching, effectively extracting the item of interest is problematic in the case of high-dimensional vectors. For example, once the index of the argmin/max is determined (e.g., giving an encryption of the one-hot encoding of that index), one has to perform a dot-product for each component of the vector to retrieve, component by component, the encrypted vector. Scaling abilities are thus limited to very small models (~ 1000 parameters at most), which is definitely not representative of modern deep neural networks. This

trade-off between the heavy dependence on the model size and the efficiency of implementing these methods over TFHE makes geometric approaches generally difficult to implement efficiently in the homomorphic domain. We next have a more in-depth look at three prominent geometric aggregators from the literature.

(Multi-)Krum [9]. To illustrate the above, Krum and Multi-Krum would be very difficult to implement fully in the encrypted domain. Indeed, both approaches require first selecting the $n - f$ ¹¹ nearest neighbors of each vector, then computing a score per vector based on the distances to these neighbors, and finally selecting one or more vectors of minimum score. Although *homomorphic nearest neighbors* has been shown to be practical for low-dimensional vectors [15, 80] over TFHE, the fact that this method requires multiple nearest neighbor operations at once renders the overall scheme computationally heavy. Furthermore, an additional round of selection is then required to determine the vector(s) with minimum score. Due to their two-level selection process, both Krum and Multi-Krum would thus only be practically achievable over TFHE. Even then, because TFHE offers no batching capabilities, both approaches are subject to the selection bottleneck and cannot be expected to scale to large models.

Minimum Diameter Averaging (MDA) [23]. This method requires solving a combinatorial optimization problem to determine the subset of vectors of size $n - f$ with minimum diameter. The average of these chosen vectors is then output by the method. From an FHE perspective, this implies distance computations, followed by three levels of argmin/argmax computations (nearest neighbors, diameter, subset selection), and terminated by an averaging operation. This renders the computations even more expensive than Krum.

Geometric Median (GM) [17]. Computing the geometric median requires solving a continuous optimization problem, most likely via an iterative algorithm. As such, it involves a prohibitive number of homomorphic operations. Additionally, the most well-known approximation method for GM, namely the Smoothed Weiszfeld algorithm [56], uses a ciphertext-vs-ciphertext division that cannot be escaped.

B.2 Coordinate-wise Aggregators

Coordinate-wise aggregators are intrinsically batching-friendly since all vector coordinates can be processed independently. These approaches are therefore a priori promising candidates to be implemented over BGV or any-other batching-able FHE scheme. In fact, their homomorphic evaluation would scale well to large models, thanks to both the SIMD parallelism available in each ciphertext and the fact that many such ciphertexts can be straightforwardly processed in parallel. However, all presently known batching-friendly cryptosystems have generally higher computational complexities than TFHE when implementing comparisons and min/max operators. So, the computational times are expected to exhibit a higher sensitivity to the number of nodes.

Coordinate-Wise Median (CWMED) [73]. Median calculations have recently been studied over batching-friendly cryptosystems [36]. However, computing a median even over a small number

of values requires large computational times. For example, [36] reports that a median over 16 8-bit vectors of size 9352 takes around 1 hour. The *amortized* time per component appears more reasonable ($\approx 0.38s$). These results are promising (by FHE standards) and hint that more practical computational times may be obtained using further optimizations, as well as by decreasing the precision of the vectors and/or the number of values involved in the calculation.

Coordinate-Wise Trimmed Mean (CWTM) [73]. This method performs a coordinate-wise sorting and then averages the $(n - 2f)$ coordinates between positions f and $n - f - 1$. Specifically, given n vectors x_0, \dots, x_{n-1} of dimension d , CWTM sorts the n vectors per coordinate to obtain $\bar{x}_0, \dots, \bar{x}_{n-1}$ satisfying

$$\bar{x}_0^{(j)} \leq \dots \leq \bar{x}_{n-1}^{(j)} \quad 0 \leq j \leq d - 1, \quad (16)$$

and returns the vector y such that

$$y = \frac{1}{n - 2f} \sum_{i=f}^{n-f-1} \bar{x}_i \quad (17)$$

This operator should not be much more costly than CWMED, since the selection is replaced by an averaging over statically selected coordinates and summation is generally a low-cost homomorphic operation. Note that since divisions are quite impractical in the homomorphic domain, the averaging operation in CWTM can be replaced by a homomorphic summation followed by a post-decryption division on the nodes' side. Indeed, there is no added value in terms of security to perform the division prior to the decryption.

Remark on CWTM vs CWMED. Be it for the trimmed mean or the median, the algorithm in the encrypted domain requires to sort the values and compute their ranks. Since data-dependent branching is not possible in a homomorphic setting, this implies that all pairs of values must be compared, thus yielding quadratic complexity. Also, in both algorithms, the rank of all elements must be homomorphically determined in order to decide which ones enter the final computation. In other words, both algorithms exhibit the same computational complexity and multiplicative depth.

Mean around Median (MeaMed) [71]. Although similar to the two previous operators, this algorithm is much more difficult to perform in the encrypted domain as it requires to compute a coordinate-wise average over the $n - f$ closest values to the median (per coordinate). That is, contrary to CWTM and CWMED, the selection criterion of the coordinates involved in the average is not static (equivalent to an $n - f$ nearest neighbors in one dimension), significantly increasing the volume and complexity of the required homomorphic computations compared to the previous two operators.

B.3 Takeaway

Following the above discussion, from an HE execution viewpoint, our qualitative analysis a priori favors the coordinate-wise methods CWTM and CWMED to be the most promising. They are expected to scale better in terms of model size over batching-friendly schemes compared to the geometric approaches. Fortunately, from an ML viewpoint, these two popular methods have been shown to provide state-of-the-art Byzantine robustness [26, 38, 39]. Furthermore, CWTM has been shown to be empirically and theoretically superior to CWMED in [4]. As such, we choose in this work to achieve

¹¹Recall that n is the total number of nodes, and f is the number of Byzantine nodes.

Byzantine resilience via a homomorphic implementation of CWTM over the BGV cryptosystem.

C Proof of (12)

Since $\text{Comp}(v, v; i, i) = 0$ for any i , we see that $0 \leq rk_i \leq n - 1$. We wish to show that $rk_i \neq rk_j$ for $i \neq j$ so that the rk_i 's are a reordering of the indices $i = 0$ through $n - 1$.

In case $v_i < v_j$, $\{i\} \cup \{k: v_k < v_i\} \subseteq \{k: v_k < v_j\}$ so that

$$\begin{aligned} rk_i &= \sum_{k=0}^{n-1} \mathbf{1}(v_i > v_k) + \sum_{k=i+1}^{n-1} \mathbf{1}(v_i == v_k) \\ &< \sum_{k=0}^{n-1} \mathbf{1}(v_j > v_k) \\ &\leq \sum_{k=0}^{n-1} \mathbf{1}(v_j > v_k) + \sum_{k=i+1}^{n-1} \mathbf{1}(v_j == v_k) \\ &= rk_j \end{aligned} \quad (18)$$

and in case $v_i == v_j$ we have $\{k: v_k == v_i\} \neq \{k: v_k == v_j\}$ so that $rk_i \neq rk_j$.

D Additional Information on Experimental Setup

D.1 Dataset Distribution

In this section, we present pictorial representations of the data heterogeneity induced in our experiments on MNIST and Fashion-MNIST. Indeed, we present in Figure 2 the distribution of class labels across honest nodes when $\alpha = 1$ (left) and 5 (right). Recall that α is the parameter of the Dirichlet distribution (see Section 6.1).

D.2 Model Architectures

To present the architecture of the models used, we employ the following compact notation used in [4, 26].

L(#inputs, #outputs) represents a **fully-connected linear layer**, R stands for **ReLU activation**, S stands for **log-softmax**, C(#in_channels, #out_channels) represents a **fully-connected 2D-convolutional layer** (kernel size 5, padding 0, stride 1), and M stands for **2D-maxpool** (kernel size 2).

The architectures of the models used on MNIST, Fashion-MNIST, and CIFAR-10 are thus the following:

- MNIST: L(784, 100) - R - L(100, 10) - S
- Fashion-MNIST: C(1, 20) - R - M - C(20, 50) - R - M - L(800, 500) - R - L(500, 10) - S
- CIFAR-10: C(3, 20) - R - M - C(20, 200) - R - M - L(5000, 120) - R - L(120, 84) - R - L(84, 10)

E Setting the Clamp Parameter

In this section, we discuss the importance of appropriately setting the value of the clamp parameter C in Algorithm 2. Figures 3 and 4 show the performance of SABLE ($\delta = 2$ bits) in terms of learning accuracy depending on the clamp parameter C . We consider the heterogeneous MNIST dataset with $\alpha = 1$, in a cross-silo system

composed of $n = 15$ nodes among which $f = 3$ are Byzantine. We vary $C \in \{10^{-5}, 0.0001, 0.001, 0.01, 0.1\}$.

It is clear that the value of C significantly affects the performance of SABLE. Clamping too low at $C = 10^{-5}$ or too high at $C = 0.1$ (i.e., potentially not clamping at all) does not help in mitigating Byzantine attacks. In this case, SABLE struggles to learn consistently against all attacks. Furthermore, looking at Figures 3 and 4, we can see that setting $C = 0.001$ (i.e., the value used in our experiments, see Section 6.1) yields the best results across all Byzantine attacks. Indeed, we can see that SABLE with $C = 0.001$ is the most robust solution among all considered algorithms since it consistently reaches the highest accuracy against all attacks, almost matching the performance of DSGD in the non-Byzantine setting (refer to Figure 6). Moreover, SABLE with $C = 0.001$ is also the fastest algorithm to converge. In fact, it only takes roughly 300 steps for SABLE to converge to its maximal accuracy under all attacks when $C = 0.001$, while it takes many more steps for the algorithm to reach desirable accuracies for other C values (e.g., 1000 steps for $C = 1e - 5$, or 600 steps for $C = 0.0001$ against ALIE). This discussion shows the criticality of appropriately setting the value of the clamp parameter C , and suggests that a hyperparameter optimization phase might be needed prior to the deployment of SABLE in practice.

F Additional Experimental Results

In this section, we complete the experimental results that could not be placed in the main paper. Figures 5 and 6 show the performance of SABLE on MNIST with $f = 3$ and 5, respectively. Figure 9 presents our results on CIFAR-10 when $f = 3$. Finally, Figures 7 and 8 test our algorithm on the Fashion-MNIST dataset when $f = 3$ and 5, respectively. These additional plots convey exactly the same observations made in Section 6.2.

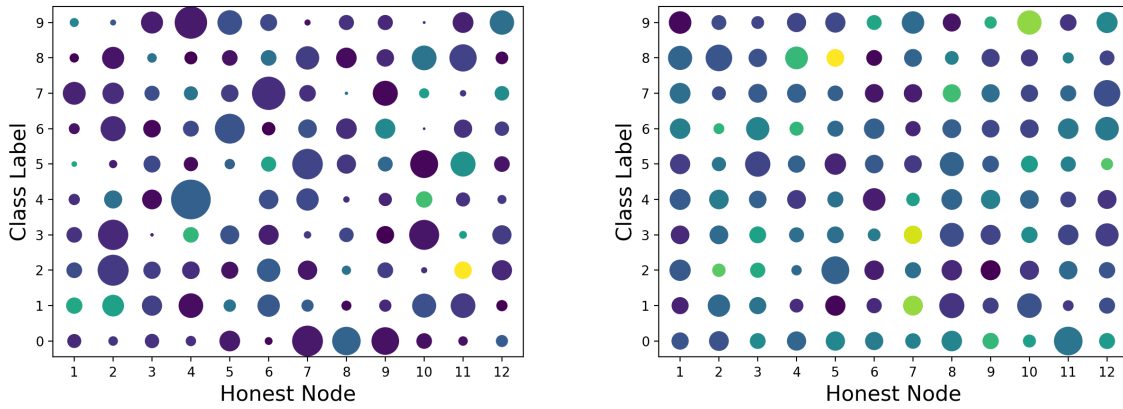


Figure 2: Distribution of data samples across honest nodes and class labels on MNIST (left) and Fashion-MNIST (right) when sampling from a Dirichlet distribution of parameter $\alpha = 1$ (left) and $\alpha = 5$ (right).

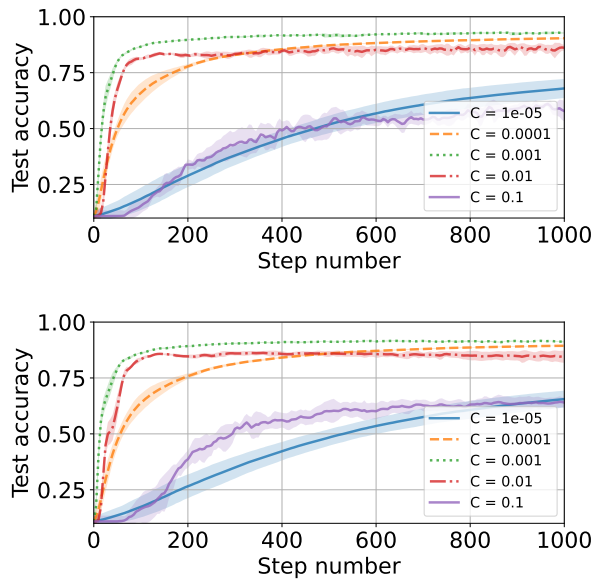


Figure 3: Performance of SABLE depending on clamp parameter C on MNIST with $\alpha = 1$ and $f = 3$ Byzantine nodes among $n = 15$. The Byzantine nodes execute the FOE (left), ALIE (right).

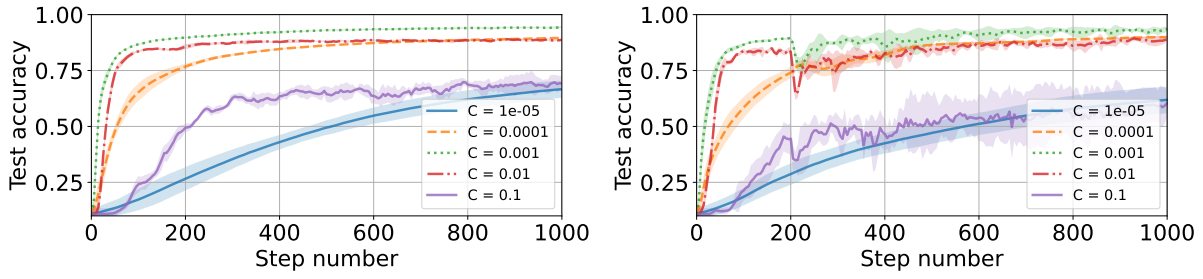


Figure 4: Performance of SABLE depending on clamp parameter C on MNIST with $\alpha = 1$ and $f = 3$ Byzantine nodes among $n = 15$. The Byzantine nodes execute the LF (left), and Mimic (right) attacks.

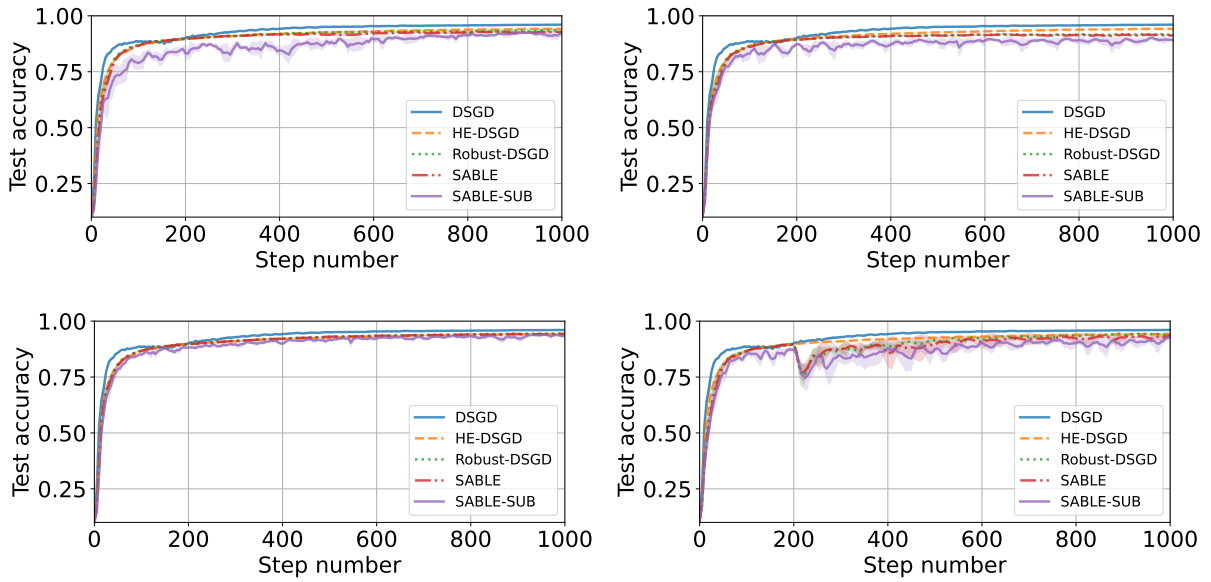


Figure 5: Experiments on heterogeneous MNIST with $\alpha = 1$ and $f = 3$ Byzantine nodes among $n = 15$. The Byzantine nodes execute the FOE (row1, left), ALIE (row 1, right), LF(row 2, left), and Mimic (row 2, right) attacks.

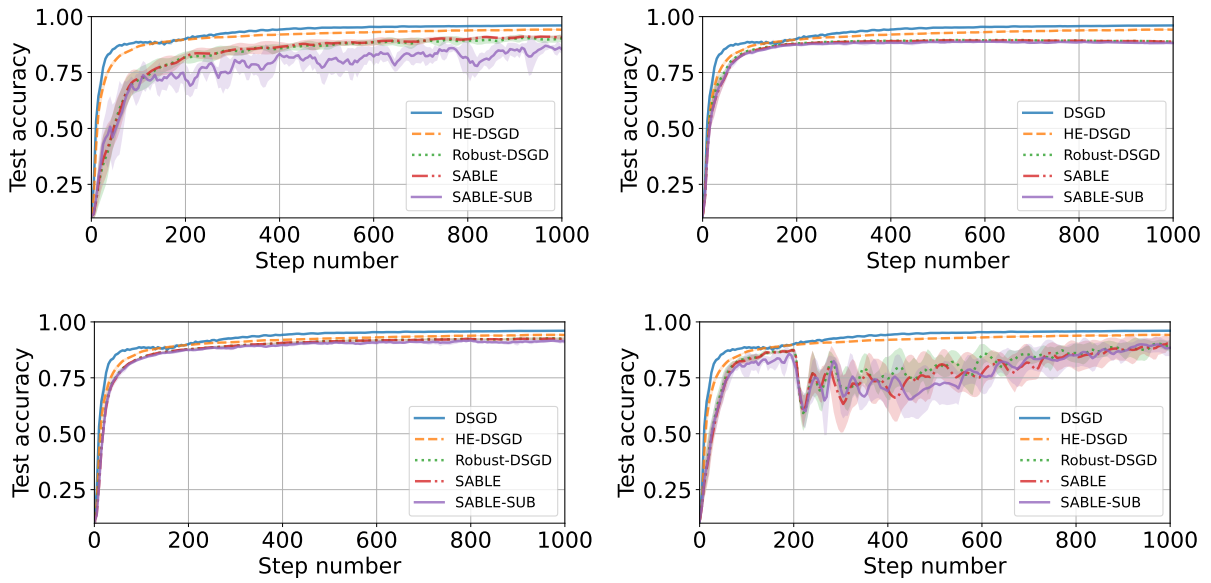


Figure 6: Experiments on heterogeneous MNIST with $\alpha = 1$ and $f = 5$ Byzantine nodes among $n = 15$. The Byzantine nodes execute the FOE (row1, left), ALIE (row 1, right), LF(row 2, left), and Mimic (row 2, right) attacks.

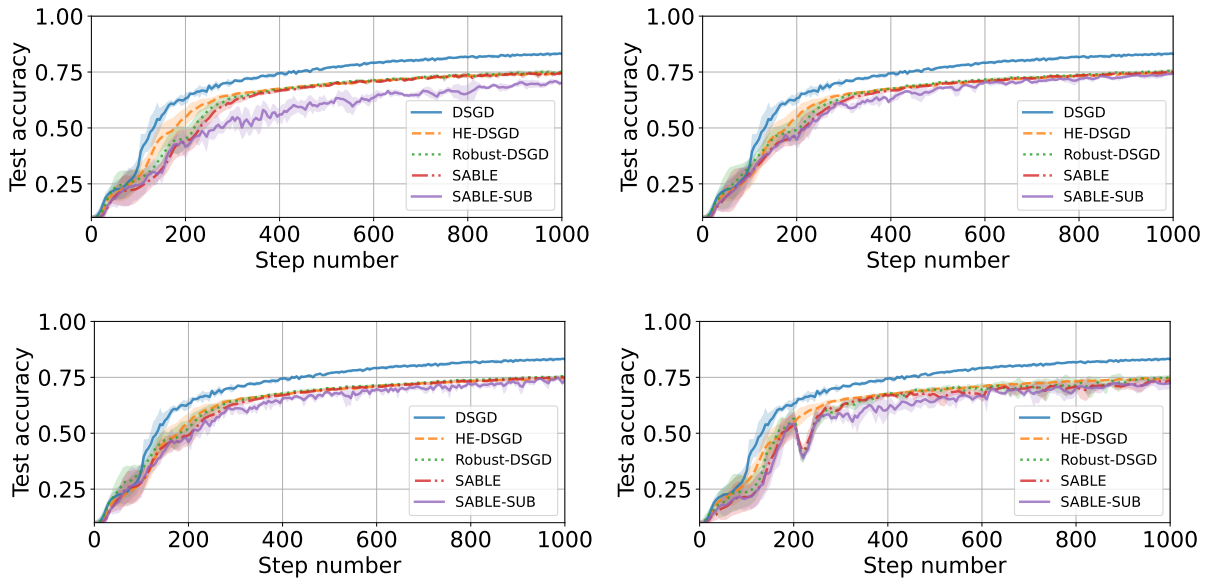


Figure 7: Experiments on heterogeneous Fashion-MNIST with $\alpha = 5$ and $f = 3$ Byzantine nodes among $n = 15$. The Byzantine nodes execute the FOE (row1, left), ALIE (row 1, right), LF(row 2, left), and Mimic (row 2, right) attacks.

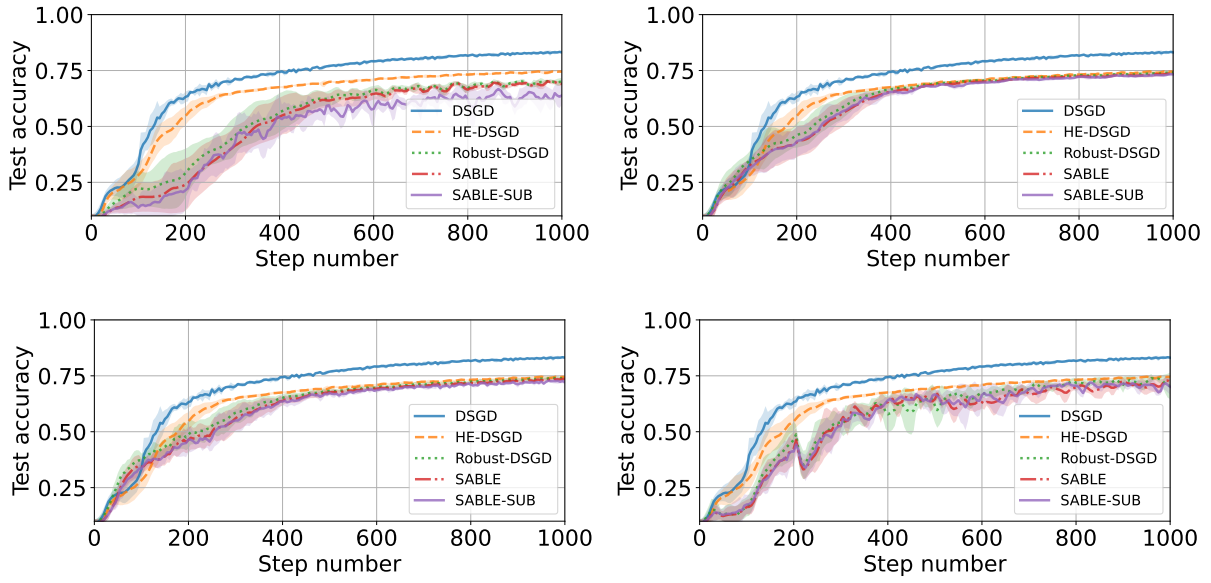


Figure 8: Experiments on heterogeneous Fashion-MNIST with $\alpha = 5$ and $f = 5$ Byzantine nodes among $n = 15$. The Byzantine nodes execute the FOE (row1, left), ALIE (row 1, right), LF(row 2, left), and Mimic (row 2, right) attacks.

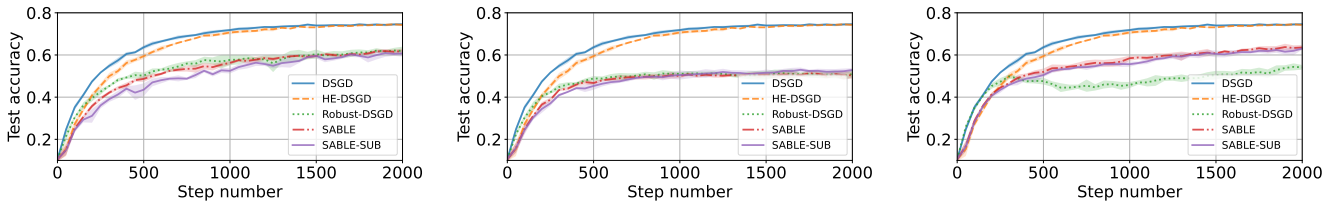


Figure 9: Experiments on CIFAR-10 with $f = 3$ Byzantine nodes among $n = 9$. The Byzantine nodes execute the FOE (left), ALIE (centre), and LF (right) attacks.